Naval Research Laboratory

Washington, DC 20375-5320

NRL/MR/6770--92-7155

Survey of Nuclear Activations for Intense Proton and Deuteron Beams

FRANK C. YOUNG

Pulsed Power Physics Branch
Plasma Physics Division

AND

DAVID V. ROSE

JAYCOR
Vienna, VA 22180-2270

December 24, 1992

REPORT DOCUMENTATION PAGE

Form Approved
OMB No. 0704-0188

1. AGENCY USE ONLY (*Leave Blank*)	2. REPORT DATE	3. REPORT TYPE AND DATES COVERED
	December 24, 1992	Interim

4. TITLE AND SUBTITLE

Survey of Nuclear Activations for Intense Proton and Deuteron Beams

5. FUNDING NUMBERS

SNL F.A.O. No. AA-9158
under DOE Contract No.
DE-04-76-DP00789

6. AUTHOR(S)

Frank C. Young and David V. Rose*

7. PERFORMING ORGANIZATION NAME(S) and ADDRESS(ES)

Naval Research Laboratory
Washington, DC 20375-5320

8. PERFORMING ORGANIZATION REPORT NUMBER

NRL/MR/6670--92-7155

9. SPONSORING/MONITORING AGENCY NAME(S) AND ADDRESS(ES)

Sandia National Laboratories
Albuquerque, NM 87185

10. SPONSORING/MONITORING AGENCY REPORT NUMBER

11. SUPPLEMENTARY NOTES

*JAYCOR, Vienna, VA 22180-2270

12a. DISTRIBUTION/AVAILABILITY STATEMENT

Approved for public release; distribution unlimited.

12b. DISTRIBUTION CODE

13. ABSTRACT (*Maximum 200 words*)

Proton- and deuteron-induced nuclear reactions which produce radioactivities are surveyed for application to experiments with intense ion beams from pulsed power generators. Positive Q-value reactions with up to 10-MeV protons or deuterons on carbon, aluminum, titanium-alloy, steel, and brass targets are identified. For each radioactivity, the half-life and decay products are tabulated. Measured cross sections from the published literature are used to identify reaction yields. For protons, thick-target yields are evaluated for (p,n) reactions on these targets. For deuterons, thick-target yields are evaluated for several (d,n), (d,p) and (d,α) reactions on these targets.

14. SUBJECT TERMS

Proton-induced nuclear reactions; Deuteron-induced nuclear reactions;
Intense proton beam; Intense deuteron beam;
Radioactive products

15. NUMBER OF PAGES

48

16. PRICE CODE

17. SECURITY CLASSIFICATION OF REPORT	18. SECURITY CLASSIFICATION OF THIS PAGE	19. SECURITY CLASSIFICATION OF ABSTRACT	20. LIMITATION OF ABSTRACT
UNCLASSIFIED	UNCLASSIFIED	UNCLASSIFIED	UL

NSN 7540-01-280-5500

Standard Form 298 (Rev. 2-89)
Prescribed by ANSI Std 239-18
298-102

CONTENTS

SURVEY OF NUCLEAR ACTIVATIONS FOR INTENSE PROTON AND DEUTERON BEAMS

I. Introduction

Nuclear reactions induced by light-ion beams which lead to radioactive products are of interest to pulsed-power experiments on the Sabre generator at Sandia National Laboratories. Light-ion beams (proton, deuteron or lithium) may be accelerated through 0 to 10 MV on this generator. Radioactivities induced in the commonly used materials, carbon, aluminum, steel, and brass may pose a radiological hazard. Because a titanium alloy is used in the ion-diode region of the Sabre generator, radioactivity induced by reactions in this alloy are also considered. Radioactivities induced by lithium ions in these targets have already been surveyed.[1] In this report, radioactive products from proton and deuteron beams incident on carbon, aluminum, titanium-alloy, steel, and brass targets are identified. For these singly-charged ion beams, incident energies of up to 10 MeV are considered.

Nuclear reactions on these targets which lead to radioactive nuclei are identified. Proton- and deuteron-induced reactions leading to the following products are considered: n, p, d, t, ^{3}He, and α. Both positive and negative Q-value reactions are included. The tabulation of Keller et al.[2] is used as a guide to identify the more energetically favorable reactions. Tabulated Q-values are based on mass excesses from Ref. 3. Positive Q-value reactions are allowed by kinematics for any bombarding energy. Negative Q-value reactions have a threshold energy given by $(M_1+M_2)(-Q)/M_2$ where M_1 is the incident projectile mass and M_2 is the target mass.

For each reaction, the residual nucleus and its decay properties are tabulated. Reactions which produce the long-lived isotopes ^{53}Mn ($T_{\frac{1}{2}} = 3.7\times10^6$ yr), ^{59}Ni ($T_{\frac{1}{2}} = 8\times10^4$ yr), and ^{63}Ni ($T_{\frac{1}{2}} = 10^2$ yr) are not included in this survey. Unrealistically large ion-beam fluences would be required to produce significant activities of these long-lived isotopes. The decay modes are

Manuscript approved November 17, 1992.

identified as β^- for electron decay, β^+ for positron decay, and ε for electron capture. Both β^+ and ε are listed when these decay modes are of comparable intensity. For β-decay, E_β is the end-point energy of the β-spectrum, and E_γ is the energy of the most intense γ-ray(s) associated with the decay. The decay modes, halflives, end-point energies and γ-ray energies are taken from Ref. 4. The most intense γ-decays are identified from Ref. 5.

Measured cross sections for some of these reactions were found in the published literature. Compilations in Ref. 6 were used to locate published sources prior to 1976. Compilations in Ref. 7 were used to locate additional sources. The computerized catalog DIALOG[8] was used for the period from 1976 to 1992. Since DIALOG does not include all the journals of interest in this time period, Physics Abstracts was used to supplement this survey. No attempt was made to incorporate cross sections from unpublished technical reports. Cross sections determined from residual activities, rather than prompt particle emissions, are the desired quantities. In many cases, excitation functions (cross sections as a function of incident proton energy) are determined by measuring delayed radioactivities induced in stacked foils. For reactions where sufficient excitation functions are available, the cross sections are combined with known stopping cross sections[9] to determine thick-target yields. Graphs of thick-target yield versus incident ion energy are included in this report.

Reactions on carbon are discussed in Sec. II. Reactions on aluminum are discussed in Sec. III. Proton-induced reactions on titanium alloy, steel, and brass are discussed in Sec. IV. Deuteron-induced reactions on these alloy targets are discussed in Sec. V. For the alloy targets, only isotopes for which the product of the isotopic abundance and the alloy proportion exceeds 1% are included because these isotopes are expected to be the primary sources of radioactivity.

II. Carbon Target

Nuclear reactions on carbon leading to radioactive products

are listed in Table I. A natural carbon target consists of two isotopes, ^{12}C and ^{13}C, with the abundances given in Table I. For thick-target calculations, the target is assumed to be natural-abundance carbon. A brief discussion of each reaction listed in Table I follows.

$^{12}C(p,\gamma)^{13}N$: The thick-target yield for this reaction below 3 MeV is determined by resonances at 457 keV and 1.70 MeV.[10] A graph of the thick-target yield is given in Fig. 1. Above 3 MeV, the ^{13}N activity from the $^{13}C(p,n)$ reaction exceeds the $^{12}C(p,\gamma)$ activity even though the isotopic abundance of ^{13}C in natural carbon is only 1.1%. For a plasma source with a natural deuterium abundance (0.015%) operating in the space-charge-limited regime, the ^{13}N activity from the $^{12}C(d,n)$ reaction for deuterons above 1.3 MeV exceeds the (p,γ) reaction yield.[10]

$^{13}C(p,n)^{13}N$: The threshold for this reaction is 3.25 MeV. The thick-target yield in Figs. 1 and 2 is based on measured cross sections.[11] It should be noted that the ^{13}N activity can also be produced by the $^{16}O(p,\alpha)^{13}N$ reaction with comparable cross sections[12] for proton energies above 7 MeV.

$^{12}C(d,n)^{13}N$: The threshold for this reaction is 0.33 MeV.[13] The thick-target yield from 2 to 5 MeV has been reported for a natural carbon target,[14] and this yield has been extended to lower energies using measured relative cross sections.[10] The measured cross sections of Wilkinson[15] were used to extend the thick-target yield to 10 MeV. The thick-target yield for this reaction is given in Figs. 1 and 2. This reaction is the most prolific source of radioactivity for a carbon target over the energy range of interest.

$^{13}C(d,p)^{14}C$: This reaction was not seriously considered in this survey for three reasons. First, the small natural abundance of ^{13}C reduces the radioactivity from this reaction by two orders of magnitude for a natural carbon target. Second, the activity will be small because the ^{14}C halflife is long, e.g., it takes more radioactive nuclei to produce a given activity for a longer halflife. Third, the ^{14}C decay produces only a low energy β-particle which is easily shielded.

Table I

Radioactivities Induced by Protons or Deuterons on Carbon and Aluminum

Target		Nuclear Reaction		Residual Nucleus			
Isotope	Abundance	Reaction	Q-Value (MeV)	Decay Mode	Half Life	E_β (MeV)	E_γ (MeV)
^{12}C	98.9%	$^{12}C(p,\gamma)^{13}N$	+1.94	β^+	10 min	1.20	0.51
		$^{12}C(d,n)^{13}N$	-0.28	β^+	10 min	1.20	0.51
^{13}C	1.1%	$^{13}C(p,n)^{13}N$	-3.00	β^+	10 min	1.20	0.51
		$^{13}C(d,p)^{14}C$	+5.95	β^-	5.7 yr	0.16	-
^{27}Al	100%	$^{27}Al(p,n)^{27}Si$	-5.59	β^+	4.2 s	3.8	0.51
		$^{27}Al(p,d)^{26}Al$	-10.8	β^+,ε	6.4 s	3.21	0.51
		$^{27}Al(d,p)^{28}Al$	+5.51	β^-	2.24 min	2.86	1.78
		$^{27}Al(d,\alpha p)^{24}Na$	-5.36	β^-	15.0 hr	1.39	2.75 1.37
		$^{27}Al(d,2p)^{27}Mg$	-4.06	β^-	9.45 min	1.77	0.844

III. Aluminum Target

Nuclear reactions on aluminum leading to radioactive products are also listed in Table I. Aluminum consists of a single isotope, ^{27}Al. The target is assumed to be 100% aluminum for thick-target calculations. A brief discussion of each reaction in Table I follows.

$^{27}Al(p,n)^{27}Si$: The reaction threshold is 5.8 MeV. The thick-target yield in Fig. 3 is based on measured cross sections.[16]

$^{27}Al(p,d)^{26}Al$: The threshold for this reaction is 11.6 MeV. No activity is possible for proton energies below 10 MeV.

$^{27}Al(d,p)^{28}Al$: The cross section for this reaction is not well known. A best fit to cross sections measured in three different experiments (Refs. 17, 18 and 19) was used to generate a thick-target yield to 5 MeV for this reaction.[20] This best-fit cross section curve is shown in Fig. 4, and the thick-target yield is given in Fig. 3. Cross sections from Ref. 19 were used to extend this yield curve to 10 MeV. Two more recent cross section measurements[21,22] are much larger than the best fit from Ref. 20, as shown in Fig. 4. The reason for the large differences (x160 at 3 MeV and x4 at 6.8 MeV) is not known. The values in Ref. 21 (0.6 to 3.2 MeV) are based on thick-target measurements and are much larger than (d,p) cross sections on other nuclei in this mass range.[7] In a thick target, additional ^{28}Al activity may be produced by the $^{27}Al(n,\gamma)^{28}Al$ reaction induced by neutrons from the $^{27}Al(d,n)^{28}Si$ reaction in the same target. This process may account for the large cross sections in Refs. 21 and 22. This process was shown to be negligible for the measurements in Ref. 19.

$^{27}Al(d,\alpha p)^{24}Na$: The kinematic threshold for this reaction is 5.8 MeV, but measured excitation functions[22,23] for this reaction indicate that the cross section is small below 10 MeV. Therefore no significant activity is expected from this reaction.

$^{27}Al(d,2p)^{27}Mg$: The kinematic threshold for this reaction is 4.4 MeV, but measured cross sections[22,24] indicate that the yield is small below 10 MeV. Therefore, no thick-target yield was evaluated for this reaction.

IV. Proton-Induced Radioactivities in the Alloy Targets

For the medium-weight nuclei in titanium-alloy, steel, and brass targets, radioactivities are produced typically by either (p,n) or (p,α) reactions. Radioactivities produced by these reactions are identified, and reaction yields are briefly discussed for constituent elements of these alloys. Thick-target yields for these targets are not reduced by the alloy composition since these may change from one material to another.

A. Titanium-Alloy Target

The titanium 6-4 alloy used in the ion-diode region of the Sabre generator consists of 90%-titanium, 6%-aluminum and 4%-vanadium. Titanium consists of five stable isotopes with abundances ranging from 5% to 74%, while vanadium is 99.8% ^{51}V. Radioactivity produced by irradiation of the aluminum in this alloy was discussed in Sec. III. Proton-induced reactions on titanium and vanadium leading to radioactive products are listed in Table II. A brief discussion of the (p,n) and (p,α) reactions in Table II follows.

(p,n) Reactions: The threshold for the (p,n) reaction on ^{46}Ti is 8.0 MeV. Immediately above threshold, ^{46}V activity has been measured,[25] but the cross section was not reported. The (p,n) reactions on ^{47}Ti and ^{48}Ti have lower thresholds of 3.78 and 4.90 MeV, respectively, and their cross sections have been measured.[26] Smooth fits were made to these cross sections, and thick-target yields based on these cross sections are presented in Fig. 5 for a natural-abundance titanium target. These reactions are primary sources of radioactivity from the proton bombardment of titanium. To produce significant activation of the long-lived ^{49}V isotope by the $^{49}Ti(p,n)$ reaction, extremely large proton fluences would be required. Furthermore, ^{49}V decays only by electron capture so its radiation hazard is minimal. For vanadium, the threshold for the (p,n) reaction is 1.56 MeV, and cross sections for this reaction have been determined from 3.1 to 10.4 MeV by measuring ^{51}Cr activity[27] and from 1.6 to 4.5 MeV by measuring neutron emission.[28] Independent measurements with

Table II

Radioactivities Induced by Protons on Titanium and Vanadium

Target		Nuclear Reaction		Residual Nucleus			
Isotope	Abundance	Reaction	Q-Value (MeV)	Decay Mode	Half Life	E_β (MeV)	E_γ (MeV)
^{46}Ti	8.0%	^{46}Ti(p,n)^{46}V	-7.85	β^+	0.43 s	6.04	0.51
		^{46}Ti(p,α)^{43}Sc	-3.09	β^+	3.89 hr	1.20	0.51
^{47}Ti	7.5%	^{47}Ti(p,n)^{47}V	-3.70	β^+	31 min	1.90	0.51
		^{47}Ti(p,α)^{44}Sc	-2.25	β^+	3.93 hr	1.47	1.16
^{48}Ti	73.7%	^{48}Ti(p,n)^{48}V	-4.80	β^+,ε	16.0 da	0.70	1.31 0.98
^{49}Ti	5.5%	^{49}Ti(p,n)^{49}V	-1.39	ε	331 da	-	-
		^{49}Ti(p,α)^{46}Sc	-1.94	β^-	83.8 da	0.36	1.12 0.89
^{50}Ti	5.3%	^{50}Ti(p,α)^{47}Sc	-2.24	β^-	3.41 da	0.44	0.16
^{51}V	99.8%	^{51}V(p,n)^{51}Cr	-1.53	ε	27.7 da	-	0.32

these two techniques[29] are consistent and are in agreement with the measurements in Ref. 28. Therefore, the cross sections from Ref. 27 are scaled to values in Ref. 28 to provide cross sections from 1.6 to 10.5 MeV. A smooth fit to these cross sections was used to calculate the thick-target yield presented in Fig. 6.

(p,α) Reactions: Thresholds for the (p,α) reactions on ^{46}Ti, ^{47}Ti, ^{49}Ti and ^{50}Ti range from 2.0 to 3.2 MeV. The (p,α) reaction on ^{48}Ti, the most abundant isotope, produces no radioactivity. These reactions tend to have small cross sections as described in Sec. IVB. The reactions on ^{46}Ti and ^{50}Ti have been measured by detecting α-emission, and ground-state differential cross-sections of only 0.03 to 0.4 mb/sr for 9- to 10-MeV protons have been reported.[30] For 14-MeV protons, total cross sections of 30 mb for ^{48}Ti and 25 mb for ^{51}V have been measured.[31] Because cross sections below 10 MeV are expected to be small and measured excitation functions are not available in the literature, no thick-target yields were evaluated for these reactions.

B. Steel and Brass Targets

These alloy targets contain several elements in different proportions. For this survey, a 70%-iron, 20%-chromium, 10%-nickel composition is assumed for #304 stainless steel, and a 67%-copper, 33%-zinc composition is assumed for brass. Each of these elements consists of several stable isotopes with significant fractional abundances. Proton-induced reactions leading to radioactive products are listed in Table III for a steel target and in Table IV for a brass target. A brief discussion of the reactions listed in these Tables follows.

(p,n) Reactions: Thresholds for the (p,n) reactions range from 1.65 MeV for ^{57}Fe to 9.51 MeV for ^{58}Ni. These reactions have been studied extensively and their cross sections increase rapidly from zero at threshold to relatively large values (10^2-10^3 mb) a few MeV above threshold. For chromium, two activities are produced: the 5.6-da ground state and a 21-min isomer. The symbol ^{52m}Mn in Tables III and VI refers to an isomeric state where ^{52}Mn is the ground state. Thick-target yields for the (p,n) reaction on ^{52}Cr, calculated using cross sections from

Table III

Radioactivities Induced by Protons on Chromium, Iron and Nickel

Target		Nuclear Reaction		Residual Nucleus			
Isotope	Abundance	Reaction	Q-Value (MeV)	Decay Mode	Half Life	E_β (MeV)	E_γ (MeV)
^{52}Cr	83.8%	$^{52}Cr(p,n)^{52}Mn$	-5.49	ε,β^+	5.6 da	0.57	1.434 0.94 0.74
		$^{52}Cr(p,n)^{52m}Mn$	-5.87	β^+	21 min	2.63	1.434
		$^{52}Cr(p,\alpha)^{49}V$	-2.60	ε	331 da	-	-
^{54}Fe	5.8%	$^{54}Fe(p,n)^{54}Co$	-9.03	β^+	1.5 min	4.3	0.51
		$^{54}Fe(p,\alpha)^{51}Mn$	-3.12	β^+	46 min	2.2	0.51
^{56}Fe	91.7%	$^{56}Fe(p,n)^{56}Co$	-5.36	ε,β^+	78 da	1.46	0.847
^{57}Fe	2.1%	$^{57}Fe(p,n)^{57}Co$	-1.62	ε	271 da	-	0.122
		$^{57}Fe(p,\alpha)^{54}Mn$	+0.24	ε	312 da	-	0.835
^{58}Ni	68.3%	$^{58}Ni(p,n)^{58}Cu$	-9.35	β^+	3.2 s	7.5	1.45
		$^{58}Ni(p,\alpha)^{55}Co$	-1.35	β^+,ε	17.9 hr	1.5	0.51
^{60}Ni	26.1%	$^{60}Ni(p,n)^{60}Cu$	-6.91	β^+	23 min	3.77	1.76 1.33
		$^{60}Ni(p,\alpha)^{57}Co$	-0.27	ε	271 da	-	0.122

Table IV

Radioactivities Induced by Protons on Copper and Zinc

Target		Nuclear Reaction		Residual Nucleus			
Isotope	Abundance	Reaction	Q-Value (MeV)	Decay Mode	Half Life	E_β (MeV)	E_γ (MeV)
^{63}Cu	69.1%	$^{63}Cu(p,n)^{63}Zn$	-4.15	β^+	38 min	2.34	0.51
		$^{63}Cu(p,d)^{62}Cu$	-8.62	β^+	9.8 min	2.93	0.51
^{65}Cu	30.9%	$^{65}Cu(p,n)^{65}Zn$	-2.13	ε	244 da	-	1.115
		$^{65}Cu(p,d)^{64}Cu$	-7.69	β^-	12.8 hr	0.575	-
				ε,β^+	12.8 hr	0.656	0.51
		$^{65}Cu(p,\alpha d)^{61}Co$	-6.76	β^-	1.65 hr	1.24	0.068
		$^{65}Cu(p,\alpha\alpha)^{57}Mn$	-7.35	β^-	1.6 min	2.56	0.122
^{64}Zn	48.9%	$^{64}Zn(p,n)^{64}Ga$	-7.85	β^+	2.6 min	6.05	0.51
		$^{64}Zn(p,\alpha)^{61}Cu$	+0.85	β^+,ε	3.4 hr	1.22	0.51
^{66}Zn	27.8%	$^{66}Zn(p,n)^{66}Ga$	-5.96	β^+,ε	9.5 hr	4.15	0.51
		$^{66}Zn(p,d)^{65}Zn$	-8.81	ε	244 da	-	1.115
^{68}Zn	18.6%	$^{68}Zn(p,n)^{68}Ga$	-3.70	β^+	68 min	1.90	0.51

Refs. 27, 32, and 33, is presented in Fig. 7. For iron, (p,n) cross sections are taken from Ref. 26 for ^{57}Fe and from Ref. 34 for ^{56}Fe. The cross sections from Ref. 34 below 10 MeV fit smoothly onto the cross sections from Ref. 35 above 10 MeV. A precise threshold measurement has been reported for the (p,n) reaction on ^{54}Fe, (Ref. 36) but no cross sections were found in the literature. The 9.20-MeV threshold for this reaction suggests that little activity can be expected below 10 MeV. Thick-target yields for the ^{56}Fe(p,n) and ^{57}Fe(p,n) reactions are given in Fig. 8. For nickel, little activation is expected below 10 MeV. Activity from the (p,n) reaction on Ni^{58} is limited by the 9.51-MeV threshold. The thick-target yield for the (p,n) reaction on ^{60}Ni, calculated from cross sections in Ref. 37, is presented in Fig. 9. For copper, a seminal study of the (p,n) cross sections for ^{63}Cu and ^{65}Cu may be found in Ref. 38, and thick-target yields based on these cross sections are given in Fig. 10. For zinc, (p,n) cross sections were taken from Ref. 39 for ^{64}Zn, and from Refs. 39-41 for ^{66}Zn and ^{68}Zn. Smooth fits were made to these cross sections, and thick-target yields based on these cross sections are presented in Fig. 11.

(p,α) reactions: No excitation functions were found in the literature for chromium, iron, or copper targets for proton energies below 9 MeV. Above 9 MeV, excitation functions have been determined for a variety of targets by measuring emitted α-particles,[42-44] rather than residual radioactivities. These (p,α) studies indicate that this reaction proceeds by a compound-nucleus process where the incident proton penetrates the Coulomb barrier of the target nucleus and excites the target. The density of nuclear excited states is large for these medium weight nuclei so that a statistical treatment of the compound nucleus is appropriate. The α-particle emission is described by an α-particle preformation coefficient in the nucleus and by Coulomb barrier transmission to exit the nucleus. Since the Coulomb barrier in this mass range is about 6.5 MeV for protons and about 13 MeV for α-particles, (p,α) cross sections should be small below 10 MeV. At 10 MeV, modest cross sections (31 mb for copper, 29 mb for zinc, 9 mb for iron, and 5 mb for chromium)

have been reported.[42,43] The $^{64}Zn(p,\alpha)$ cross section has been determined from 8 to 22 MeV by measuring residual radioactivity.[45] Despite the positive Q-value of this reaction, the cross section is only 17 mb at 8 MeV and increases to a maximum of 80 mb at 15 MeV. For nickel, thick-target yields to produce ^{55}Co and ^{57}Co activities, calculated using cross sections from Ref. 46, are presented in Fig. 9. For all these (p,α) reactions, the excitation functions decrease rapidly with decreasing energy as expected from Coulomb-barrier-penetration considerations. A similar argument applies to the $^{65}Cu(p,\alpha\alpha)$ and $^{65}Cu(p,\alpha d)$ reactions.

(p,d) reactions: These reactions on copper and zinc have large negative Q-values. Experiments indicate that these reactions are not common for medium-weight elements.[47] On the other hand, (p,pn) reactions are commonly observed. These reactions require an additional 2.22 MeV which corresponds to thresholds greater than 10 MeV for the (p,pn) reactions on ^{65}Cu and ^{66}Zn.

V. Deuteron-Induced Radioactivities in the Alloy Targets

For the medium-weight elements in the titanium-alloy, steel, and brass targets, a specific radioactivity may be produced by several different deuteron-induced reactions. Therefore, it is difficult to associate a measured radioactivity with one nuclear reaction. Consequently, only a limited number of excitation functions for deuteron-induced reactions have been measured for these elements. Furthermore, the (d,n), (d,p) and (d,α) reactions all have positive Q-values and cross sections on the order of 100 mb above the Coulomb barrier. For deuterons in the few MeV range (below the Coulomb barrier), the (d,α) reactions have appreciably smaller cross sections than the (d,n) and (d,α) reactions.[48] Substantial radioactivities can be expected from these reactions, and the following discussion will focus on these reactions. Deuteron-induced reactions leading to radioactivities are identified, and activation yields are briefly discussed for these alloy targets.

A. Titanium-Alloy Target

Deuteron-induced reactions on titanium and vanadium in the titanium alloy target which lead to radioactive products are listed in Table V. For titanium, there are four isotopes with abundances of 5% to 8%, while ^{48}Ti is 74% abundant. Cross sections for the ^{47}Ti(d,n) reaction and for the (d,α) reactions on ^{46}Ti, ^{48}Ti and ^{49}Ti have been determined in the range from 5.5 to 10 MeV,[49] but these measurements are insufficient to evaluate thick-target yields. These cross sections increase monotonically up to 10 MeV with values at 10 MeV of 130 mb for the (d,n) reaction and 40 to 80 mb for the (d,α) reactions. For the bombardment of a natural titanium target with 6.5-MeV deuterons, a thick-target yield of 8.3×10^{-5} ^{48}V/deuteron has been reported for producing ^{48}V activity.[50] This activity includes both the ^{47}Ti(d,n)^{48}V and ^{48}Ti(d,2n)^{48}V reactions. Cross sections for several of the negative Q-value reactions on titanium are negligible below 5 MeV and increase rapidly with energy from 5 and 10 MeV. For example, the ^{47}Ti(d,2n)^{47}V reaction cross section is negligible at 5.5 MeV, but approaches 200 mb at 10 MeV.[49] A similar behavior is observed for the ^{48}Ti(d,2n)^{48}V reaction.[51] The (d,n) and (d,α) reactions on the most abundant ^{48}Ti isotope lead to rather long-lived isotopes so large activities are not expected for these reactions. Shorter half-life activities are produced by these reactions on the other isotopes, however these activities are reduced by the smaller isotopic abundances. Consequently, the activation of titanium by deuterons is not as large as for some other target materials.

For vanadium, the most likely source of radioactivity is the positive Q-value ^{51}V(d,p)^{52}V reaction. Cross sections for this reaction, based on proton measurements, are 11 mb at 3.8 MeV and 17 mb at 4.5 MeV.[52] Even larger cross sections can be expected for the activation of ^{52}V because these proton measurements include only higher-energy emitted protons. Thick-target yields for producing ^{51}Cr by deuteron bombardment of vanadium has been reported.[53] This yield is nearly zero at 5 MeV and increases monotonically to 2.3×10^{-4} ^{51}Cr/deuteron at 10 MeV. This activity is attributed to the ^{51}V(d,2n)^{51}Cr reaction. No other

Table V

Radioactivities Induced by Deuterons on Titanium and Vanadium

Target		Nuclear Reaction		Residual Nucleus			
Isotope	Abundance	Reaction	Q-Value (MeV)	Decay Mode	Half Life	E_β (MeV)	E_γ (MeV)
^{46}Ti	8.0%	^{46}Ti(d,n)^{47}V	+2.95	β^+	31 min	1.90	0.51
		^{46}Ti(d,t)^{45}Ti	-6.94	β^+	3.08 hr	1.04	0.51
		^{46}Ti(d,α)^{44}Sc	+4.40	β^+	3.93 hr	1.47	1.16
		^{46}Ti(d,2p)^{46}Sc	-3.81	β^-	83.8 da	0.36	1.12 0.89
		^{46}Ti(d,αn)^{43}Sc	-5.31	β^+	3.89 hr	1.20	0.51
^{47}Ti	7.5%	^{47}Ti(d,n)^{48}V	+4.61	β^+,ε	16.0 da	0.70	1.31 0.98
		^{47}Ti(d,^{3}He)^{46}Sc	-4.97	β^-	83.8 da	0.36	1.12 0.89
		^{47}Ti(d,2p)^{47}Sc	-2.04	β^-	3.41 da	0.44	0.16
		^{47}Ti(d,2n)^{47}V	-5.92	β^+	31 min	1.90	0.51
		^{47}Ti(d,αn)^{44}Sc	-4.47	β^+	3.93 hr	1.47	1.16
^{48}Ti	73.7%	^{48}Ti(d,n)^{49}V	+4.52	ε	331 da	-	-
		^{48}Ti(d,^{3}He)^{47}Sc	-5.95	β^-	3.41 da	0.44	0.16
		^{48}Ti(d,α)^{46}Sc	+3.98	β^-	83.8 da	0.36	1.12 0.89
		^{48}Ti(d,2p)^{48}Sc	-5.42	β^-	43.7 hr	0.65	1.31 1.04 0.98
		^{48}Ti(d,2n)^{48}V	-7.02	β^+,ε	16.0 da	0.70	1.31 0.98
		^{48}Ti(d,αp)^{45}Ca	-4.25	β^-	163 da	0.26	-
		^{48}Ti(d,2α)^{42}K	-5.18	β^-	12.4 hr	3.52	1.53

Continued on next page.

Table V Continued

Radioactivities Induced by Deuterons on Titanium and Vanadium

Target		Nuclear Reaction		Residual Nucleus			
Isotope	Abundance	Reaction	Q-Value (MeV)	Decay Mode	Half Life	E_β (MeV)	E_γ (MeV)
^{49}Ti	5.5%	$^{49}Ti(d,^3He)^{48}Sc$	-5.85	β^-	43.7 hr	0.65	1.31 1.04 0.98
		$^{49}Ti(d,\alpha)^{47}Sc$	+6.48	β^-	3.41 da	0.44	0.16
		$^{49}Ti(d,2p)^{49}Sc$	-3.45	β^-	57 min	2.00	-
		$^{49}Ti(d,\alpha n)^{46}Sc$	-4.16	β^-	83.8 da	0.36	1.12 0.89
		$^{49}Ti(d,2\alpha)^{43}K$	-3.69	β^-	22.2 hr	0.83	0.62 0.37
^{50}Ti	5.3%	$^{50}Ti(d,p)^{51}Ti$	+4.16	β^-	5.8 min	2.14	0.32
		$^{50}Ti(d,^3He)^{49}Sc$	-6.68	β^-	57 min	2.00	-
		$^{50}Ti(d,\alpha)^{48}Sc$	+3.79	β^-	43.7 hr	0.65	1.31 1.04 0.98
		$^{50}Ti(d,2p)^{50}Sc$	-7.91	β^-	1.7 min	3.7	1.55
		$^{50}Ti(d,\alpha n)^{47}Sc$	-4.47	β^-	3.41 da	0.44	0.16
		$^{50}Ti(d,\alpha p)^{47}Ca$	-5.66	β^-	4.54 da	0.69	1.30
		$^{50}Ti(d,2\alpha)^{44}K$	-7.79	β^-	22 min	5.66	1.16
^{51}V	99.8%	$^{51}V(d,p)^{52}V$	+5.08	β^-	3.8 min	2.5	1.43
		$^{51}V(d,2p)^{51}Ti$	-3.90	β^-	5.8 min	2.14	0.32
		$^{51}V(d,2n)^{51}Cr$	-3.76	ε	27.7 da	-	0.32
		$^{51}V(d,\alpha p)^{48}Sc$	-4.27	β^-	43.7 hr	0.65	1.31 1.04 0.98
		$^{51}V(d,2\alpha)^{45}Ca$	-3.10	β^-	163 da	0.26	-

activation cross sections have been published for deuterons on vanadium.

B. Steel Target

Deuteron-induced reactions leading to radioactive products are listed in Table VI for a steel target. For the 20%-chromium component of this target, only ^{52}Cr and ^{53}Cr have significant abundances. For natural-abundance chromium, the thick-target yield (reactions/deuteron) at 8 MeV for activating ^{52}Mn by the $^{52}Cr(d,2n)^{52}Mn$ reaction is 7× less than the thick-target yield for activating ^{51}Cr by the $^{50}Cr(d,n)^{51}Mn(\beta^-)^{51}Cr$ and $^{50}Cr(d,p)^{51}Cr$ reactions.[54] The isotopic abundance of ^{50}Cr is only 4.4%. Reactions on ^{50}Cr are not included in Table VI because the abundance of this isotope in a steel target is less than 1%, and ^{51}Cr is not expected to be a primary source of radioactivity. Above 8 MeV, the activation of ^{52}Mn increases rapidly with energy, and calculated thick-target yields for Mn^{52} and the isomer Mn^{52m}, evaluated using cross sections from Ref. 55, are presented in Fig. 12. The thick-target yield for producing ^{54}Mn by deuteron bombardment of chromium has been determined.[54] This yield increases monotonically from nearly zero at 1 MeV to 5.8×10^{-5} ^{54}Mn/deuteron at 10 MeV.

Radioactivities produced by deuteron-induced reactions on natural iron have been identified and excitation functions have been measured for deuterons above 5 MeV.[56] In the range from 5 to 10 MeV, the largest activation cross sections are for ^{55}Co, ^{57}Co, and ^{54}Mn. The cobalt activities are induced principally by the $^{54}Fe(d,n)^{55}Co$ and $^{56}Fe(d,n)^{57}Co$ reactions. Below 5 MeV, ^{55}Co activation cross sections,[57] measured over the energy range from 2.44 to 5.5 MeV, are a factor-of-two smaller than the cross sections in Ref. 56. The cross sections in Ref. 57 were used to evaluate thick-target yields because the initial deuteron energy for the stacked-foil measurements in this experiment is 5.5 MeV, compared with 40 MeV in Ref. 56. The excitation function for ^{55}Co in Ref. 56 is scaled to cross sections in Ref. 57 to give activation cross sections for ^{55}Co and ^{57}Co up to 10 MeV. The ^{54}Mn activity is produced principally by the $^{56}Fe(d,\alpha)^{54}Mn$ and

Table VI

Radioactivities Induced by Deuterons on Chromium, Iron and Nickel

Target		Nuclear Reaction		Residual Nucleus			
Isotope	Abundance	Reaction	Q-Value (MeV)	Decay Mode	Half Life	E_β (MeV)	E_γ (MeV)
^{52}Cr	83.8%	$^{52}Cr(d,t)^{51}Cr$	-5.78	ε	27.7 da	-	-
		$^{52}Cr(d,2n)^{52}Mn$	-7.78	ε,β^+	5.6 da	0.57	1.434 0.94 0.74
		$^{52}Cr(d,2n)^{52m}Mn$	-8.10	β^+	21 min	2.63	1.43
		$^{52}Cr(d,2p)^{52}V$	-3.98	β^-	3.8 min	2.5	1.43
^{53}Cr	9.5%	$^{53}Cr(d,n)^{54}Mn$	5.34	ε	312 da	-	0.835
		$^{53}Cr(d,^3He)^{52}V$	-5.64	β^-	3.8 min	2.5	1.43
		$^{53}Cr(d,2p)^{53}V$	-4.5	β^-	1.6 min	2.4	1.00
^{54}Fe	5.8%	$^{54}Fe(d,n)^{55}Co$	2.83	β^+,ε	17.9 hr	1.5	0.51
		$^{54}Fe(d,p)^{55}Fe$	7.08	ε	2.7 yr	-	-
		$^{54}Fe(d,t)^{53}Fe$	-7.36	β^+	8.5 min	2.8	0.51
		$^{54}Fe(d,\alpha)^{52}Mn$	5.17	ε,β^+	5.6 da	0.57	1.434 0.94 0.74
		$^{54}Fe(d,\alpha)^{52m}Mn$	4.79	β^+	21 min	2.63	1.43
		$^{54}Fe(d,2p)^{54}Mn$	-2.14	ε	312 da	-	0.835
^{56}Fe	91.7%	$^{56}Fe(d,n)^{57}Co$	3.80	ε	271 da	-	0.122
		$^{56}Fe(d,t)^{55}Fe$	-4.95	ε	2.7 yr	-	-
		$^{56}Fe(d,\alpha)^{54}Mn$	5.66	ε	312 da	-	0.835
		$^{56}Fe(d,2n)^{56}Co$	-7.58	ε,β^+	78 da	1.46	0.847
		$^{56}Fe(d,2p)^{56}Mn$	-5.14	β^-	2.58 hr	2.85	0.847

Continued on next page

Table VI Continued

Radioactivities Induced by Deuterons on Chromium, Iron and Nickel

Target		Nuclear Reaction		Residual Nucleus			
Isotope	Abundance	Reaction	Q-Value (MeV)	Decay Mode	Half Life	E_β (MeV)	E_γ (MeV)
^{57}Fe	2.1%	$^{57}Fe(d,n)^{58}Co$	4.73	ε,β^+	71 da	0.47	0.81
		$^{57}Fe(d,^3He)^{56}Mn$	-5.07	β^-	2.58 hr	2.85	0.847
		$^{57}Fe(d,2n)^{57}Co$	-3.84	ε	271 da	-	0.122
		$^{57}Fe(d,2p)^{57}Mn$	-4.14	β^-	1.6 min	2.56	0.122
^{58}Ni	68.3%	$^{58}Ni(d,n)^{59}Cu$	1.20	β^+	82 s	3.78	0.51
		$^{58}Ni(d,\alpha)^{56}Co$	6.51	ε,β^+	78 da	1.46	0.847
		$^{58}Ni(d,t)^{57}Ni$	-5.94	ε,β^+	36 hr	0.84	1.37
		$^{58}Ni(d,^3He)^{57}Co$	-2.68	ε	271 da	-	0.122
		$^{58}Ni(d,2p)^{58}Co$	-1.83	ε,β^+	71 da	0.47	0.81
		$^{58}Ni(d,\alpha n)^{55}Co$	-3.57	β^+,ε	17.9 hr	1.5	0.51
		$^{58}Ni(d,\alpha p)^{55}Fe$	0.67	ε	2.7 yr	-	-
		$^{58}Ni(d,2\alpha)^{54}Mn$	3.61	ε	312 da	-	0.835
^{60}Ni	26.1%	$^{60}Ni(d,n)^{61}Cu$	2.58	β^+,ε	3.4 hr	1.22	0.51
		$^{60}Ni(d,\alpha)^{58}Co$	6.08	ε,β^+	71 da	0.47	0.81
		$^{60}Ni(d,2n)^{60}Cu$	-9.13	β^+	23 min	3.77	1.33
		$^{60}Ni(d,2p)^{60}Co$	-4.26	β^-	5.27 yr	0.32	1.17 1.33
		$^{60}Ni(d,\alpha n)^{57}Co$	-2.49	ε	271 da	-	0.122

$^{54}Fe(d,2p)^{54}Mn$ reactions, and cross sections for ^{54}Mn are taken from Ref. 56. Thick-target yields for a natural iron target, calculated using these cross sections, are presented in Fig. 13.

For the 10%-nickel component in the steel target, only ^{58}Ni and ^{60}Ni have significant abundances. Excitation functions[58] for (d,n) reactions on these nuclei have been measured over the energy range from 2 to 12 MeV. These cross sections increase rapidly with energy up to peaks of 200 mb at 8 MeV for ^{58}Ni and 470 mb at 8 MeV for ^{60}Ni. Above these peaks, the cross sections decrease slowly with increasing energy. These activation cross sections are smaller than the cross sections for ^{58}Ni at 3.0, 3.5 and 4.0 MeV in Ref. 59 and larger than the cross sections for ^{60}Ni at 7.2 and 9.4 MeV in Ref. 60. Thick-target yields were evaluated using the cross sections in Ref. 58 because they encompass a broad energy range. These yields are presented in Fig. 14. Activation cross sections for the (d,α) reactions on ^{58}Ni and ^{60}Ni are smaller than the (d,n) cross sections.[60,61] The (d,α) cross sections increase monotonically with increasing deuteron energy from 5 to 10 MeV. The thick-target yield for the reaction $^{58}Ni(d,\alpha)^{56}Co$, calculated using cross sections in Refs. 60 and 61, is displayed in Fig. 14. For a natural nickel target, ^{58}Co activation may be produced by both the $^{60}Ni(d,\alpha)^{58}Co$ and $^{58}Ni(d,2p)^{58}Co$ reactions. The ^{58}Co activation in Fig. 2 of Ref. 62 is presumably due to both reactions rather than just the $^{58}Ni(d,2p)^{58}Co$ reaction. The thick-target yield for ^{58}Co activation, calculated from cross sections in Refs. 60 and 62 is presented in Fig. 14. Cross sections for the (d,t), (d,^{3}He), (d,αn), (d,αp) and (d,2α) reactions on ^{58}Ni and the (d,2n) and (d,αn) reactions on ^{60}Ni have been measured,[60-63] and activities induced by these reactions are negligible below 10 MeV.

C. Brass Target

Deuteron-induced reactions leading to radioactive products are listed in Table VII for the 67%-copper component in this target. The (d,p) and (d,2n) reactions on ^{63}Cu and ^{65}Cu are prolific sources of radioactivity for deuterons below 10 MeV. A seminal study of activations for these reactions may be found in

Table VII

Radioactivities Induced by Deuterons on Copper

Target		Nuclear Reaction		Residual Nucleus			
Isotope	Abundance	Reaction	Q-Value (MeV)	Decay Mode	Half Life	E_β (MeV)	E_γ (MeV)
^{63}Cu	69.1%	$^{63}Cu(d,p)^{64}Cu$	5.69	β^-	12.8 hr	0.575	-
				ε,β^+	12.8 hr	0.656	0.51
		$^{63}Cu(d,t)^{62}Cu$	-4.58	β^+	9.8 min	2.93	0.51
		$^{63}Cu(d,2n)^{63}Zn$	-6.37	β^+	38 min	2.34	0.51
		$^{63}Cu(d,\alpha p)^{60}Co$	-0.51	β^-	5.27 yr	0.318	1.17
							1.33
^{65}Cu	30.9%	$^{65}Cu(d,p)^{66}Cu$	4.84	β^-	5.1 min	2.63	1.04
		$^{65}Cu(d,t)^{64}Cu$	-3.65	β^-	12.8 hr	0.575	-
				ε,β^+	12.8 hr	0.656	0.51
		$^{65}Cu(d,2n)^{65}Zn$	-4.36	ε	244 da	-	1.115
		$^{65}Cu(d,2p)^{65}Ni$	-3.57	β^-	2.52 hr	2.13	1.48
		$^{65}Cu(d,\alpha p)^{62}Co$	-2.32	β^-	14 min	2.88	1.17

Ref. 64. For the (d,p) reactions, significant disagreements in the magnitude and shape of the excitation functions are observed between three independent cross-section measurements. For the (d,2n) reactions, there is good agreement between the same three experiments. Thick-target yields, based on cross sections from Ref. 64, are presented in Fig. 15. Measurements of the $^{63}Cu(d,t)^{62}Cu$ and $^{65}Cu(d,2p)^{65}Ni$ reactions[65,66] indicate that the activation cross sections for these reactions are much less than for the (d,p) and (d,2n) reactions.

For the zinc in this target, deuteron-induced reactions leading to radioactive products are listed in Table VIII. The ^{64}Zn, ^{66}Zn, and ^{68}Zn isotopes have significant abundances for the 33%-zinc component of the target. Excitation functions have been measured for the (d,p) and (d,n) reactions in Table VIII. Activation cross sections for the $^{64}Zn(d,p)^{65}Zn$ reaction include the $^{64}Zn(d,n)^{65}Ga$ reaction because the 15-min ^{65}Ga isotope decays to the 244-da ^{65}Zn isotope.[67,68] This short-lived precursor is included in delayed activation measurements of ^{65}Zn. For ^{66}Zn, cross sections[69] for the $^{66}Zn(d,n)^{67}Ga$ reaction include a small contribution from the $^{67}Zn(d,2n)^{67}Ga$ reaction at higher deuteron energy. The natural abundance of ^{67}Zn is only 4.1%. For ^{68}Zn, the (d,p) reaction produces either ^{69}Zn or the isomer, ^{69m}Zn. The isomer decays by an isomeric transition (IT) with the emission of a 0.44-MeV γ-ray to ^{69}Zn. Separate cross sections have been measured for these two activities.[70] Thick-target yields, based on cross sections from Refs. 67-70, are presented in Fig. 16.

For the (d,α) reactions in Table VIII, only the cross section for activating ^{64}Cu has been published.[71] Isotopically enriched targets were required to extract the excitation function for this activity. The more intense (d,p) and (d,n) reactions which induce competing short-lived activities make measurements of the smaller (d,α) cross sections difficult. No excitation functions have been reported for the 10-min ^{62}Cu or 5-min ^{66}Cu activities. The thick-target yield for ^{64}Cu activity, based on the cross sections in Ref. 71, is presented in Fig. 16.

Table VIII

Radioactivities Induced by Deuterons on Zinc

Target		Nuclear Reaction		Residual Nucleus			
Isotope	Abundance	Reaction	Q-Value (MeV)	Decay Mode	Half Life	E_β (MeV)	E_γ (MeV)
^{64}Zn	48.9%	$^{64}Zn(d,n)^{65}Ga$	1.72	β^+	15 min	2.24	0.51
		$^{64}Zn(d,p)^{65}Zn$	5.76	ε	244 da	-	1.115
		$^{64}Zn(d,t)^{63}Zn$	-5.60	β^+	38 min	2.34	0.51
		$^{64}Zn(d,\alpha)^{62}Cu$	7.52	β^+	9.8 min	2.93	0.51
		$^{64}Zn(d,2p)^{64}Cu$	-2.01	β^-	12.8 hr	0.575	-
				ε,β^+	12.8 hr	0.656	0.51
^{66}Zn	27.8%	$^{66}Zn(d,n)^{67}Ga$	3.05	ε	78 hr	-	0.093
		$^{66}Zn(d,t)^{65}Zn$	-4.78	ε	244 da	-	1.115
		$^{66}Zn(d,\alpha)^{64}Cu$	7.26	β^-	12.8 hr	0.575	-
				ε,β^+	12.8 hr	0.656	0.51
		$^{66}Zn(d,2p)^{66}Cu$	-4.07	β^-	5.1 min	2.63	1.04
		$^{66}Zn(d,2n)^{66}Ga$	-8.18	β^+,ε	9.5 hr	4.15	0.51
^{68}Zn	18.6%	$^{68}Zn(d,p)^{69}Zn$	4.28	β^-	57 min	0.91	-
		$^{68}Zn(d,p)^{69m}Zn$	3.84	IT	13.9 hr	-	0.44
		$^{68}Zn(d,^3He)^{67}Cu$	-4.50	β^-	62 hr	0.57	0.185
		$^{68}Zn(d,\alpha)^{66}Cu$	6.97	β^-	5.1 min	2.63	1.04
		$^{68}Zn(d,2n)^{68}Ga$	-5.93	β^+	68 min	1.90	0.51
		$^{68}Zn(d,2p)^{68}Cu$	-6.03	β^-	31 sec	3.51	1.08

Excitation functions have been measured for several of the negative Q-value reactions in Table VIII. For the $^{64}Zn(d,2p)$ reaction, the cross section is small (5 mb) at 10 MeV and negligible below 8 MeV.[71] For the $^{66}Zn(d,2n)^{66}Ga$ reaction, the cross section increases from zero at the 8.4-MeV threshold to 150 mb at 10 MeV.[70] For the $^{68}Zn(d,2n)^{68}Ga$ reaction the threshold is 6.1 MeV, but some ^{68}Ga activity is produced at lower energy from the $^{67}Zn(d,n)^{68}Ga$ reaction. The thick-target yield for ^{68}Ga activity, based on the cross sections in Ref. 70, is presented in Fig. 16.

VI. Summary

For the proton-induced reactions in this survey, radioactivities are produced primarily by (p,n) reactions. Yields for these reactions increase rapidly from threshold. Thresholds are less than 4 MeV for the carbon, titanium-alloy, steel, and brass targets and 5.8 MeV for an aluminum target. At 10 MeV, the $^{51}V(p,n)$ and $^{65}Cu(p,n)$ reactions have the largest thick-target yields ($\sim 10^{-3}$ reactions/proton); these two reactions also have the smallest thresholds. Residual activities with hour-to-day halflives resulting from the proton bombardment of aluminum, titanium, steel and brass have been measured and specific radioisotopes were identified.[72] The observed activities are consistent with the expectations from this survey.

For the deuteron-induced reactions, radioactivities are produced primarily by the (d,n), (d,p), and (d,α) reactions. The (d,α) yields are smaller than the (d,n) or (d,p) yields. Thick-target yields for the (d,n) and (d,p) reactions increase rapidly at low energy and approach 5×10^{-4} reactions/deuteron at 10 MeV. At low energy, the (d,n) yield for carbon is larger than for the other targets presumably due to the smaller Coulomb barrier. In the energy range from 8 to 10 MeV, thick-target yields for the (d,n) and (d,p) reactions are similar so differences in the yields for different targets are due primarily to the different target abundances. For some of these reactions, significant differences are found in the literature for the same reaction

cross section measured in different experiments by different researchers. In some cases, additional measurements have been reported in order to sort out these differences. However, large differences remain for the $^{27}Al(d,p)^{28}Al$ reaction, as indicated in Fig. 4. Additional measurements are needed to provide reliable cross sections for this reaction from zero to 10 MeV.

The radioactivity produced by a single intense pulse of ions can be evaluated from the thick-target yield. For a 100-kA, 100-ns duration pulse of protons or deuterons, the initial activity in Curies is given by $1.2 \times 10^6 fY(E)/T_{\frac{1}{2}}$ where f is the fractional abundance of the target element in the alloy target; Y(E) is the thick-target yield at energy E; and $T_{\frac{1}{2}}$ is the halflife of the induced radioactivity in seconds. To illustrate this evaluation, activities are determined for two reactions which have large yields. For 10-MeV protons on brass, the ^{65}Zn activity from the $^{65}Cu(p,n)$ reaction is 34 μCurie, while the ^{63}Zn activity from the $^{63}Cu(p,n)$ reaction is 0.16 Curie. The large difference in these activities is due to the shorter ^{63}Zn halflife (38 min) compared with the ^{65}Zn halflife (244 da). For 10-MeV deuterons on carbon, the ^{13}N activity from the $^{12}C(d,n)$ reaction is 0.96 Curie. These examples indicate that relatively large radioactivities can be produced by intense proton or deuteron beams under some conditions. Much smaller activities are obtained for targets which have smaller yields and produce longer halflife activities. For example, for 10-MeV protons on the titanium-alloy target, the ^{47}V and ^{48}V activities from the $^{47}Ti(p,n)$ and $^{48}Ti(p,n)$ reactions are only 13 mCurie and 0.31 mCurie, respectively. These activities are even less for lower energy protons.

In addition to radioactivity induced in the target by proton or deuteron beams, radioactivity may be induced in the target or in surrounding materials by neutrons from (p,n) or (d,n) reactions. These activities, however, are expected to be small because neutron intensities from these reactions are much less than the ion-beam intensities.

Nuclear activations provide an attractive technique for determining the properties of intense ion beams in pulsed power

experiments. Ion-beam intensities and energies can be determined by measuring delayed activations.[10] A variety of techniques have been employed including: thick-target yields from resonance reactions,[10] stacked-foil activations,[20,73,74] simultaneous activations of different target materials,[20,74] (p,n) threshold reactions,[74,75] and secondary-reaction activation.[76] For this purpose, reactions with large yields which produce short-lived activities (minute-to-hour) are usually preferred. Activations produced by the nuclear reactions on carbon and aluminum in this survey have been used to diagnose proton and deuteron beams with energies below 5 MeV. In the future, it is expected that nuclear activation techniques will be used to diagnose ion beams at higher energies where a larger choice of nuclear reactions on a variety of targets is available.

Acknowledgements

Appreciation is expressed to Dr. Richard Peacock and Ms. Harriet Oxley of the NRL Library Staff for their assistance with the DIALOG literature search. The encouragement of John Maenchen to carry out this work is appreciated. This work was supported by the Department of Energy through Sandia National Laboratories.

REFERENCES

1. F.C. Young and D.V. Rose, Survey of Radioactivities Induced by Lithium Ions, NRL Memorandum Report No. 6974, 1992.

2. K.A. Keller, J. Lange and H. Münzel, in Landbolt-Bornstein Numerical Data and Functional Relationships in Science and Technology Vol. 5, Part a, Q-Values, edited by H. Schopper (Springer-Verlag, New York, 1973).

3. J.B. Marion and F.C. Young, Nuclear Reaction Analysis (North-Holland, Amsterdam, 1968) p. 157.

4. Chart of the Nuclides, Knolls Atomic Power Laboratory, 11th Edition, April, 1972.

5. C.M. Lederer, J.M. Hollander and I. Perlman, Table of Isotopes, 6th Edition (John Wiley, New York, 1967).

6. F.K. McGowan, W.T. Milner, H.J. Kim and Wanda Hyatt, Nuclear Data Tables A6, 353 (1969); A7, 1 (1969); F.K. McGowan and W.T. Milner, Nuclear Data Tables A8, 199 (1970); 9, 469 (1971); 11, 1 (1972); Atomic Data and Nuclear Data Tables 12, 499 (1973); 15, 189 (1975); 18, 1 (1976).

7. K.A. Keller, J. Lange, H. Münzel and G. Pfennig, in Landbolt-Bornstein Numerical Data and Functional Relationships in Science and Technology Vol. 5, Part b, Excitation Functions for Charged-Particle Induced Nuclear Reactions, edited by H. Schopper (Springer-Verlag, New York, 1973).

8. DIALOG Information Services, Inc., 3460 Hillview Ave., Palo Alto, CA 94304.

9. H.H. Andersen and J.F. Ziegler, The Stopping and Ranges of Ions in Matter, Vol. 3, Hydrogen (Pergamon Press, New York, 1977).

10. F.C. Young, J. Golden and C.A. Kapetanakos, Rev. Sci. Instrum. 48, 432 (1977).

11. P. Dagley, W. Haeberli and J.X. Saladin, Nucl. Phys. 24, 353 (1961).

12. A.B. Whitehead and J.S. Foster, Can. J. Phys. 36, 1276 (1958).

13. T.W. Bonner, J.E. Evans and J.E. Hill, Phys. Rev. 75, 1398 (1949).

14. R.J. Jaszczak, R.L. Macklin and J.H. Gibbons, Phys. Rev. 181, 1428 (1969).

15. D.H. Wilkinson, Phys. Rev. 100, 32 (1955).

16. I.F. Bubb, J.M. Poate and R.H. Spear, Nucl. Phys. 65, 655 (1965).

17. E. McMillan and E.O. Lawrence, Phys. Rev. 47, 343 (1935).

18. C.S. Lin and E.K. Lin, Nuovo Cimento A 66, 336 (1970).

19. J.M. Flores, Phys. Rev. 127, 1246 (1962).

20. F.C. Young and M. Friedman, J. Appl. Phys. 46, 2001 (1975).

21. E. Schuster and K. Wohlleben, J. Appl. Rad. Isotopes 19, 471 (1968).

22. R.L. Wilson, D.J. Frantsvog and A.R. Kunselman, C. Détraz and C.S. Zaidins, Phys. Rev. C 13, 976 (1976).

23. H.F. Röhm, C.J. Verwey, J. Steyn and W.L. Rautenbach, J. Inorg. Nucl. Chem. 31, 3345 (1969).

24. R. Radicella, J. Rodriguez, G.B. Baró and O. Hittmair, Z. Physik 150, 653 (1958).

25. J. Jänecke, Phys. Lett. 6, 69 (1963).

26. S. Tanaka and M. Furukawa, J. Phys. Soc. Japan 14, 1269 (1959).

27. J. Wing and J.R. Huizenga, Phys. Rev. 128, 280 (1962).

28. J.L. Zyskind, C.A. Barnes, J.M. Davidson, W.A. Fowler, R.E. Marrs and M.H. Shapiro, Nucl. Phys. A343, 295 (1980).

29. S. Kailas, S.K. Gupta, S.S. Kerekatte and C.V. Fernandes, Pramana 24, 629 (1985).

30. H.S. Plendl, L.J. Defelice and R.K. Sheline, Nucl. Phys. 73, 131 (1965).

31. N.T. Porile, C.R. Lux, J.C. Pacer and J. Wiley, Nucl. Phys. A240, 77 (1975).

32. F. Boehm, P. Marmier and P. Preiswerk, Helv. Phys. Acta 25, 599 (1952).

33. H. Taketani and W. Parker Alford, Phys. Rev. 125, 291 (1962).

34. I.L. Jenkins and A.G. Wain, J. Inorg. Nucl. Chem. 32, 1419 (1970).

35. E. Gadioli, A.M. Grassi Strini, G. Lo Bianco, G. Strini and G. Tagliaferri, Nuovo Cimento 22A, 547 (1974).

36. S.D. Hoath, R.J. Petty, J.M. Freeman, G.T.A. Squier and W.E. Burcham, Phys. Lett. 51B, 345 (1974).

37. S. Tanaka, M. Furukawa and M. Chiba, J. Inorg. Nucl. Chem. 34, 2419 (1972).

38. R. Collé, R. Kishore and J.B. Cumming, Phys. Rev. C 9, 1819 (1974).

39. H.A. Howe, Phys. Rev. 109, 2083 (1958).

40. J.-P. Blaser, F. Boehm, P. Marmier and D.C. Peaslee, Helv. Phys. Acta 24, 3 (1951).

41. M. Hille, P. Hille, M. Uhl and W. Weisz, Nucl. Phys. A198, 625 (1972).

42. C.B. Fulmer and C.D. Goodman, Phys. Rev. 117, 1339 (1960).

43. I. Kumabe, C.L. Wang, M. Kawashima, M. Yada and H. Ogata, J. Phys. Soc. Japan 14, 713 (1959).

44. L. Milazzo Colli, G.M. Braga Marcazzan, R. Bonetti, M. Milazzo and J.W. Smits, Nuovo Cimento 39, 171 (1977).

45. B.L. Cohen, E. Newman, R.A. Charpie and T.H. Handley, Phys. Rev. 94, 620 (1954).

46. F. Tárkányi, F. Szelecsényi and P. Kopecky, Appl. Radiat. Isot. 42, 513 (1991).

47. B.L. Cohen and E. Newman, Phys. Rev. 99, 718 (1955).

48. J.H. Bjerregaard, P.F. Dahl, O. Hansen and G. Sidenius, Nucl. Phys. 51, 641 (1964).

49. K.L. Chen and J.M. Miller, Phys. Rev. 134, B1269 (1964).

50. P.P. Dmitriev, I.O. Konstantinov and N.N. Krasnov, Soviet Atomic Energy, 29, 916 (1970).

51. W.H. Burgess, G.A. Cowan, J.W. Hadley, W. Hess, T. Shull, M.L. Stevenson and H.F. York, Phys. Rev. 95, 750 (1954).

52. J.P. Schiffer and L.L. Lee, Jr., Phys. Rev. 115, 1705 (1959).

53. C.P. Dmitriev, I.O. Konstantinov and N.N. Krasnov, Soviet Atomic Energy, 29, 917 (1970).

54. P. Kafalas and J.W. Irvine, Jr., Phys. Rev. 104, 703 (1956).

55. H.I. West, Jr., R.G. Lanier and M.G. Mustafa, Phys. Rev. C 35, 2067 (1987).

56. J.W. Clark, C.B. Fulmer and I.R. Williams, Phys. Rev. 179, 1104 (1969).

57. P.P. Coetzee and M. Peisach, Radiochim. Acta 17, 1 (1972).

58. M. Cogneau, L.J. Lilly and J Cara, Nucl. Phys. A99, 686 (1967).

59. J.H. Carver and G.A. Jones, Nucl. Phys. 24, 607 (1961).

60. J. Zweit, A.M. Smith, S. Downey and H.L. Sharma, Appl. Radiat. Isot. 42, 193 (1991).

61. M. Blann and G. Merkel, Phys. Rev. 131, 764 (1963).

62. C.K. Cline, Nucl. Phys. A174, 73 (1971).

63. R. Radicella, J. Rodriguez, G.B. Baró and O. Hittmair, Z. Physik 153, 314 (1958).

64. H. Okamura and S. Tamagawa, Nucl. Phys. A169, 401 (1971).

65. C.B. Fulmer and I.R. Williams, Nucl. Phys. A155, 40 (1970).

66. J.W. Irvine, Jr., J. Chem. Soc. (London) Suppl. S356 (1949).

67. S.J. Nassiff and H. Münzel, Radiochem. Radioanal. Lett. 12, 353 (1972).

68. J.H. Carver and G.A. Jones, Nucl. Phys. 11, 400 (1959).

69. S.J. Nassiff and H. Münzel, Radiochim. Acta 19, 97 (1973).

70. L.J. Gilly, G.A. Henriet, M. Preciosa Alves and P.C. Capron, Phys. Rev. 131, 1727 (1963).

71. D.C. Williams and J.W. Irvine, Jr., Phys. Rev. 130, 265 (1963).

72. C.L. Ruiz and G.W. Cooper, in Particle Beam Fusion Progress Report 1988, Sandia Report SAND91-0225, p. 90, April, 1992.

73. J.M. Neri, J.R. Boller, P.F. Ottinger, B.V. Weber and F.C. Young, Appl. Phys. Lett. 50, 1331 (1987).

74. F.C. Young, S.J. Stephanakis and D. Mosher, J. Appl. Phys. 48, 3642 (1977).

75. F.C. Young, J.M. Neri, B.V. Weber, R.J. Commisso, S.J. Stephanakis and T.J. Renk, Ion Energy Diagnostics for Voltage Determinations in Plasma-Erosion-Opening-Switch Experiments, NRL Memorandum Report 6059, December, 1987.

76. R.J. Leeper, K.H. Kim, D.E. Hebron and N.D. Wing, Nucl. Instrum. Meth. Phys. Res. B24/25, 695 (1987).

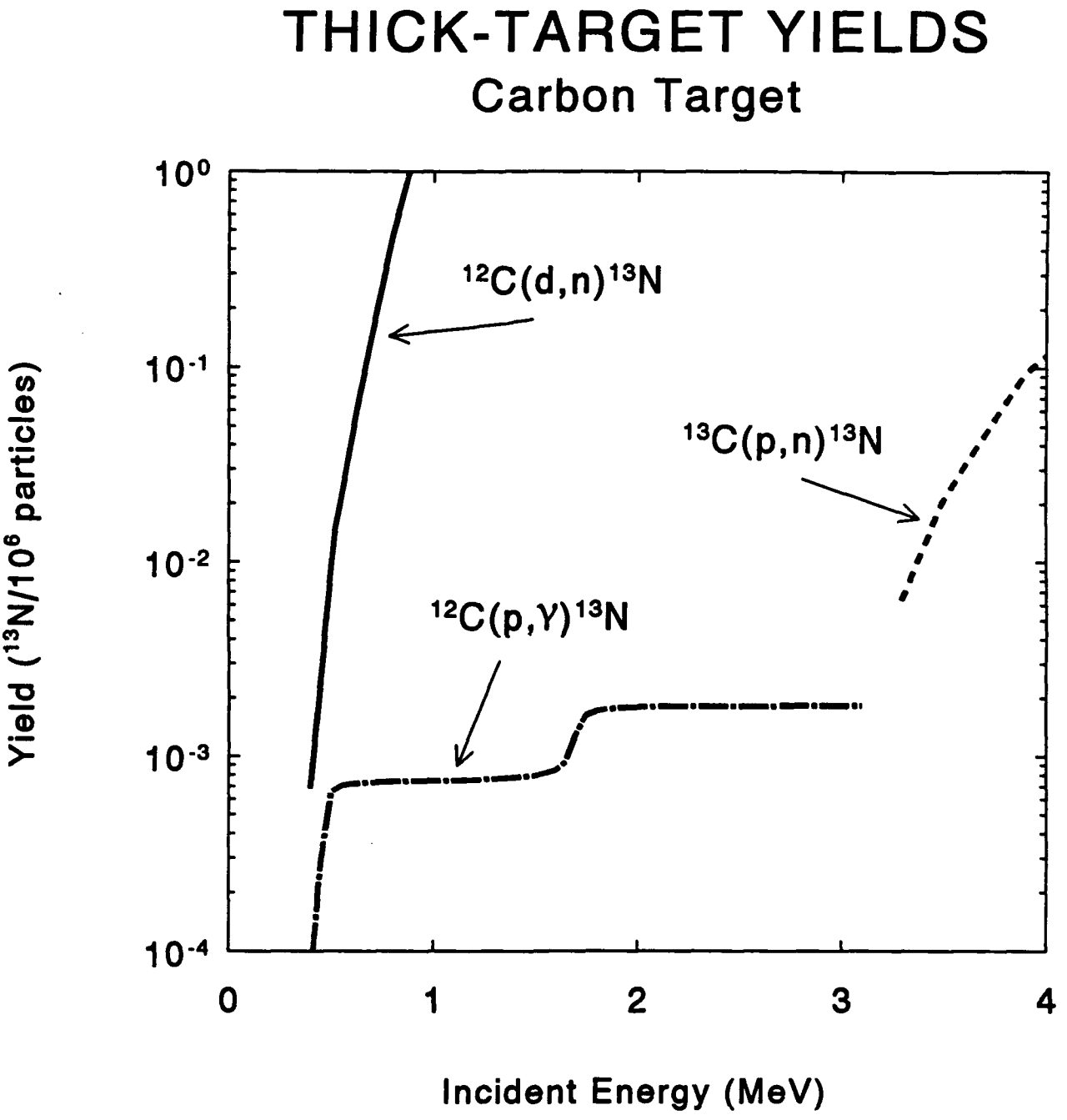

Fig. 1. Thick-target yields for the $^{12}C(p,\gamma)^{13}N$, $^{13}C(p,n)^{13}N$ and $^{12}C(d,n)^{13}N$ reactions below 4 MeV in a natural carbon target.

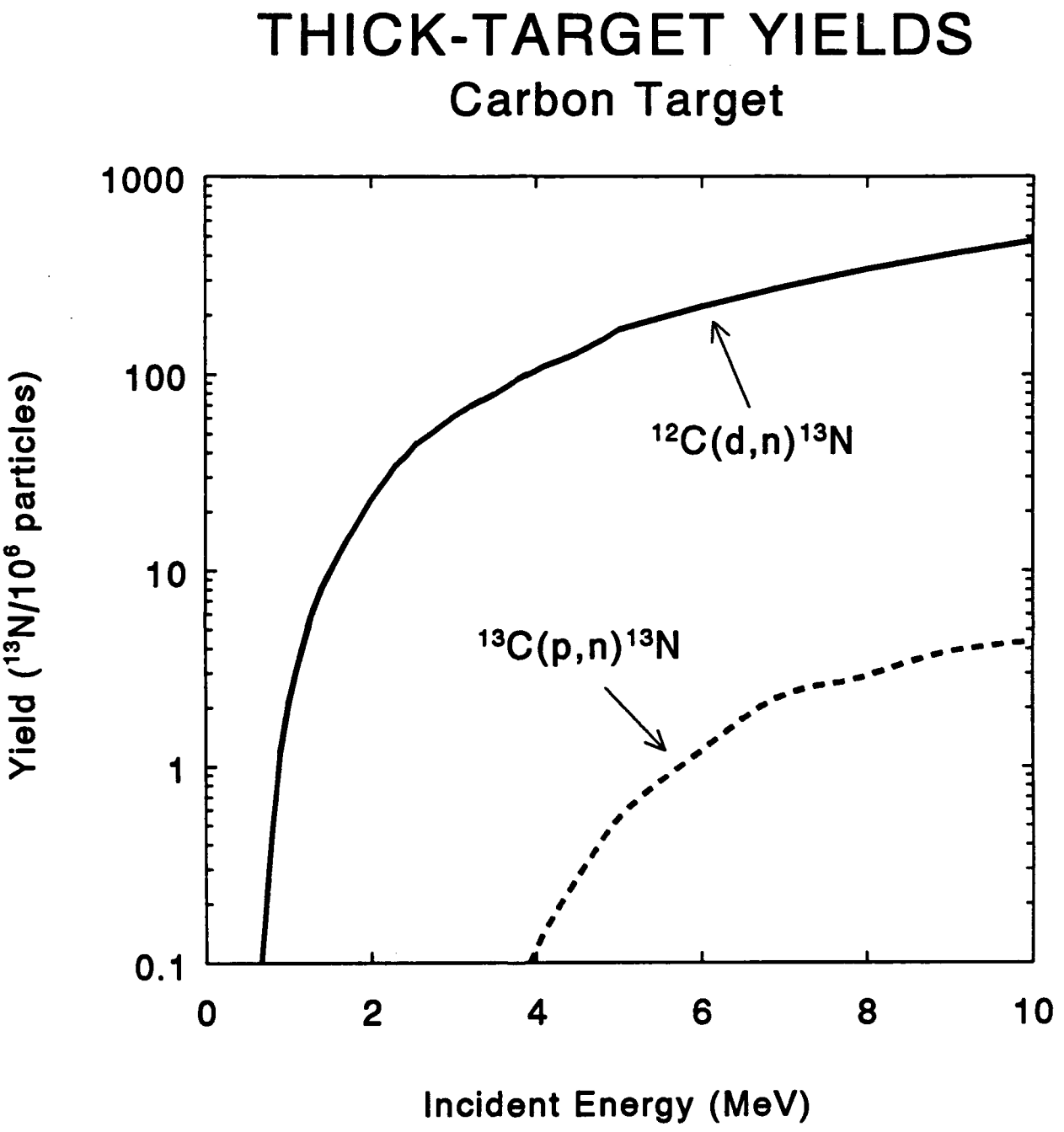

Fig. 2. Thick-target yields for the $^{13}C(p,n)^{13}N$ and $^{12}C(d,n)^{13}N$ reactions up to 10 MeV in a natural carbon target.

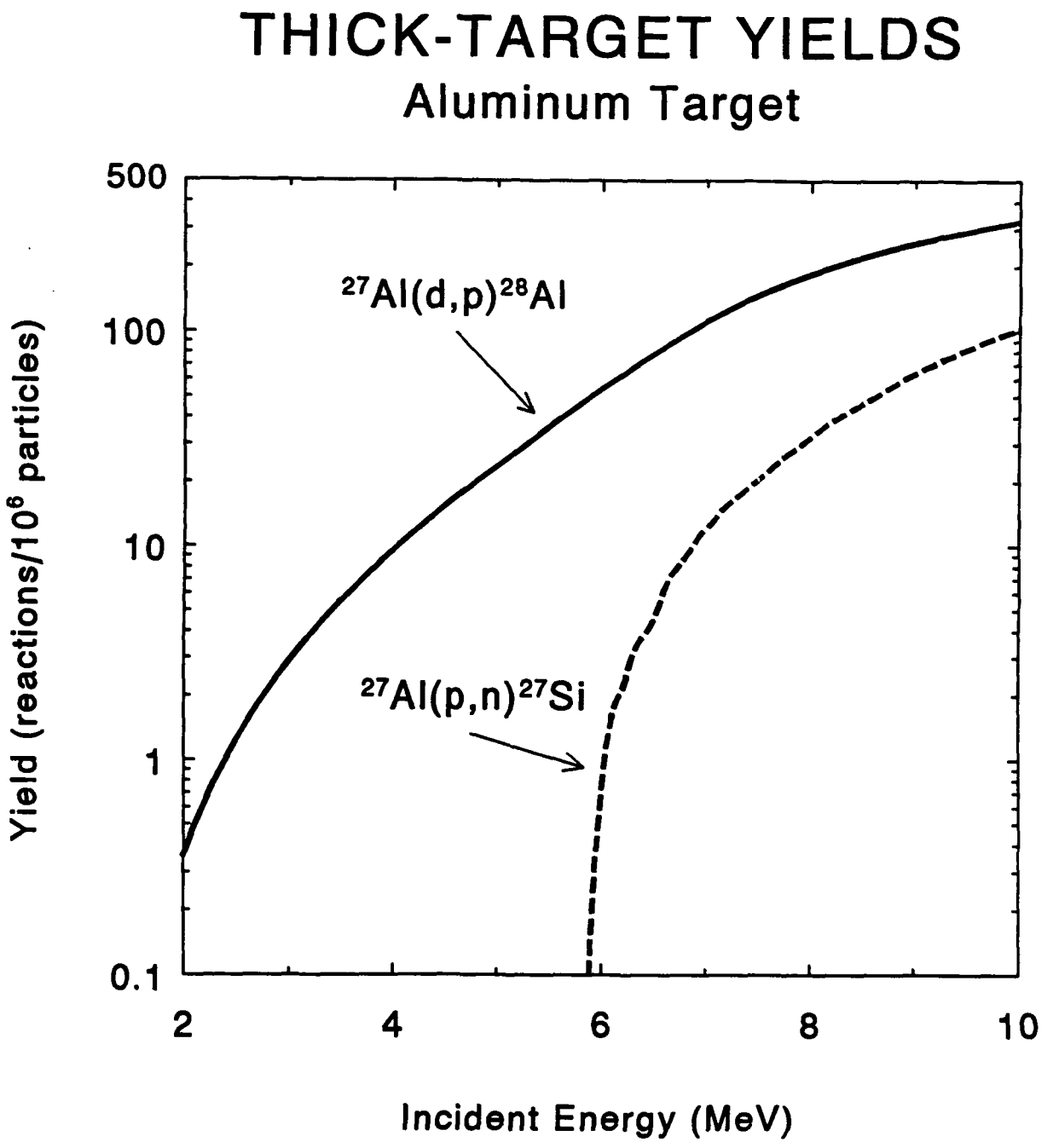

Fig. 3. Thick-target yields for the $^{27}Al(p,n)^{27}Si$ and $^{27}Al(d,p)^{28}Al$ reactions in an aluminum target.

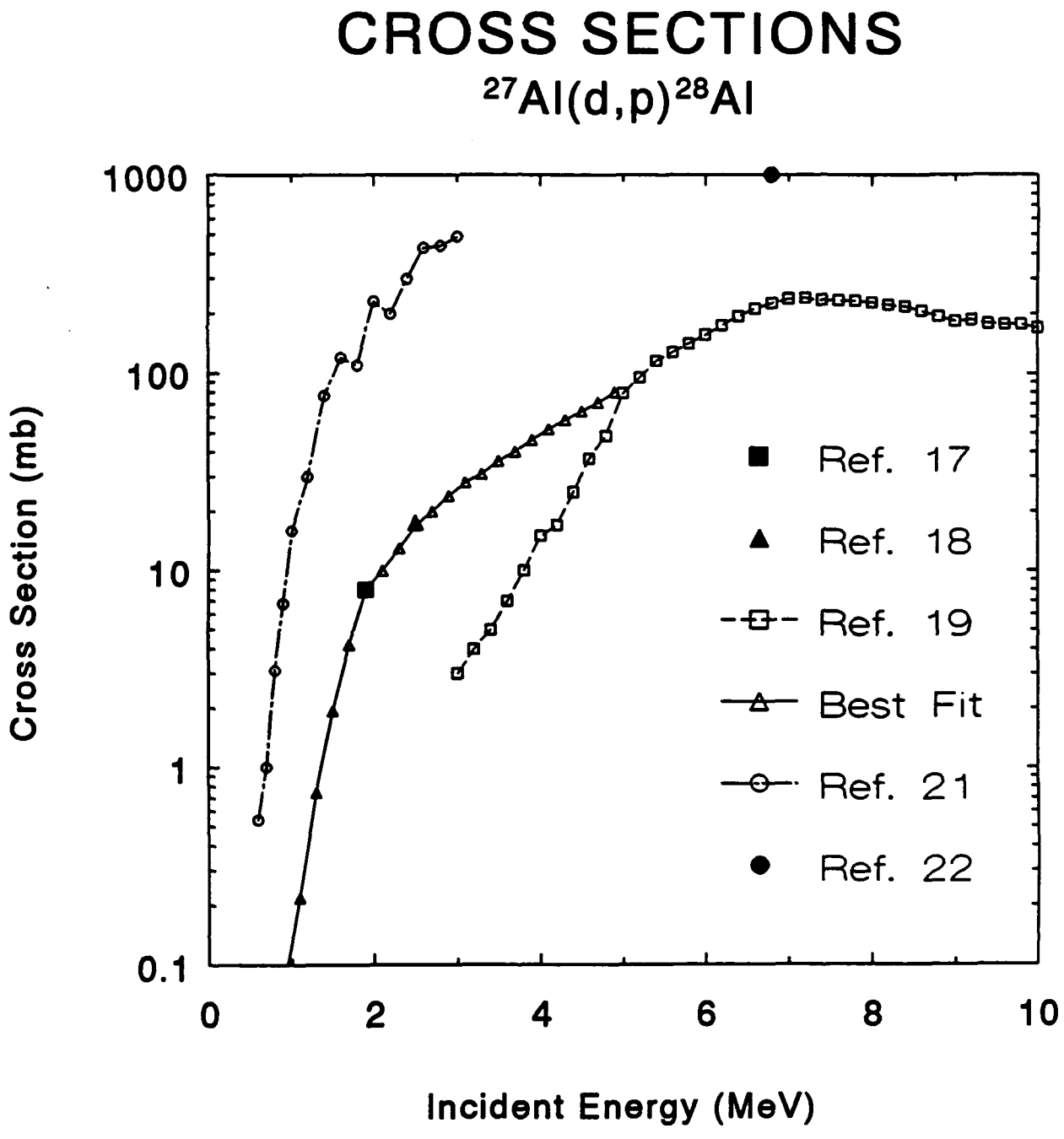

Fig. 4. Measured cross sections for the $^{27}Al(d,p)^{28}Al$ reaction. The References are identified in the text. The best fit is for cross sections from References 17, 18 and 19.

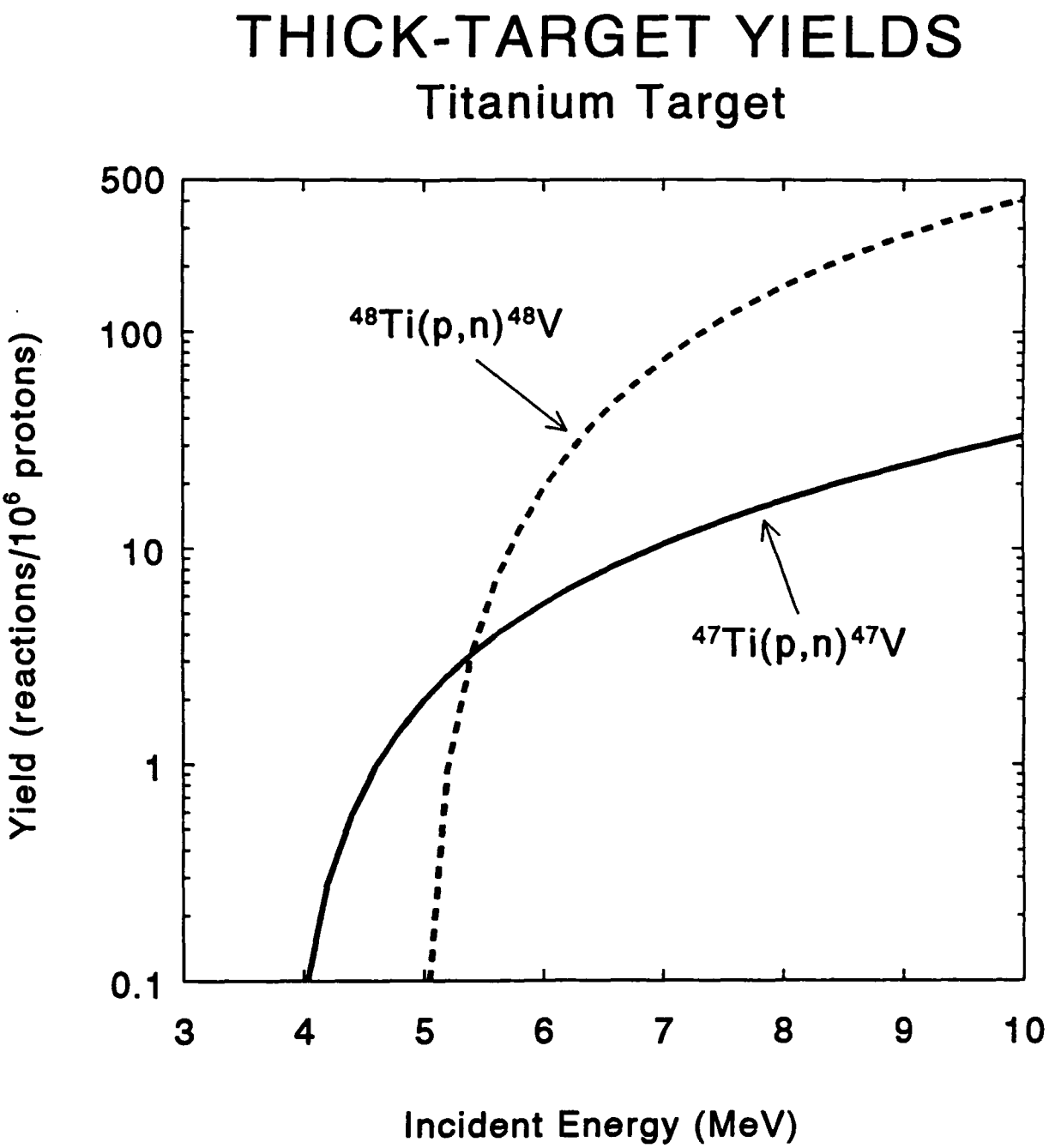

Fig. 5. Thick-target yields for the $^{47}Ti(p,n)^{47}V$ and $^{48}Ti(p,n)^{48}V$ reactions in a natural titanium target.

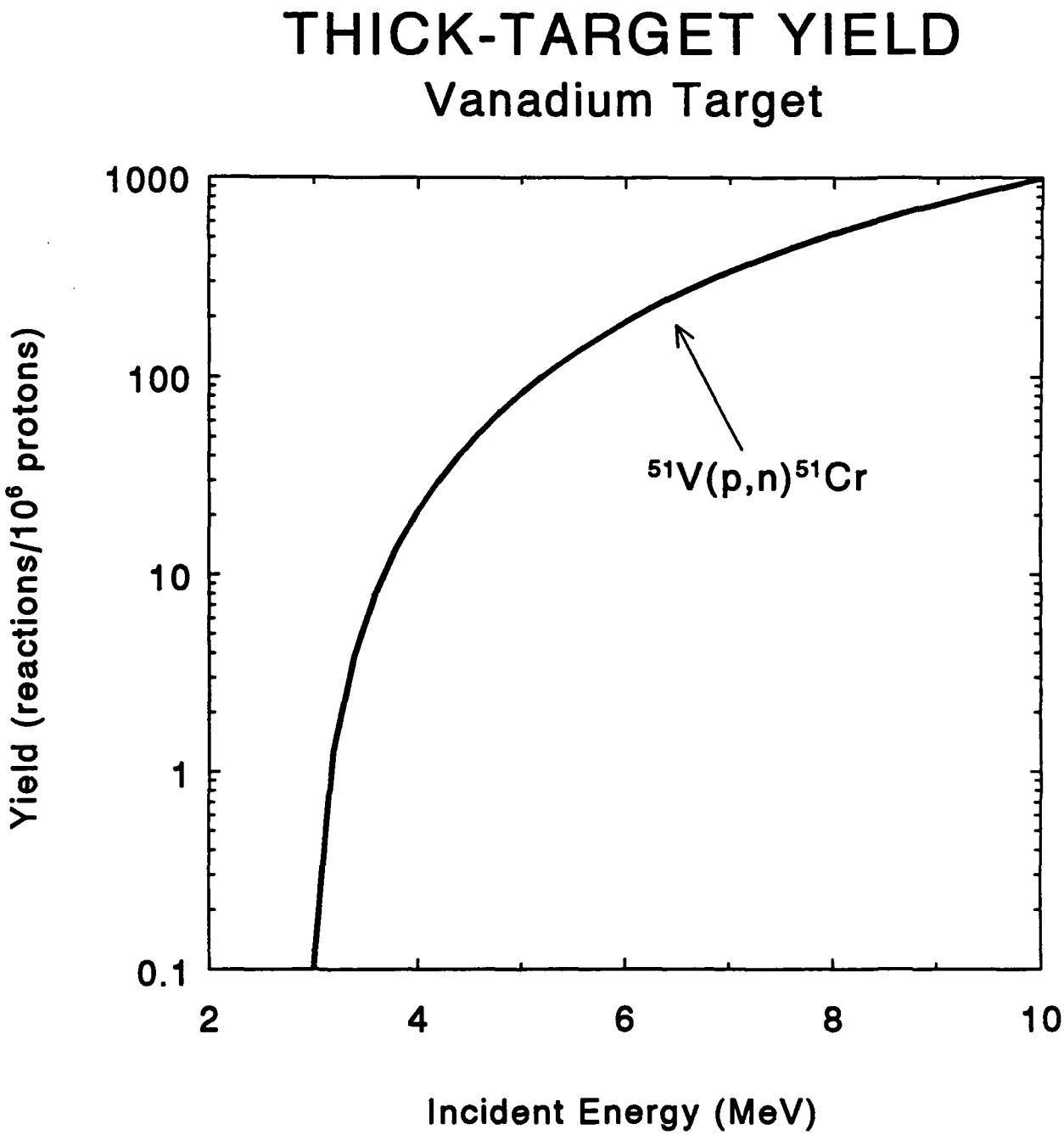

Fig. 6. Thick-target yield for the $^{51}V(p,n)^{51}Cr$ reaction in a natural vanadium target.

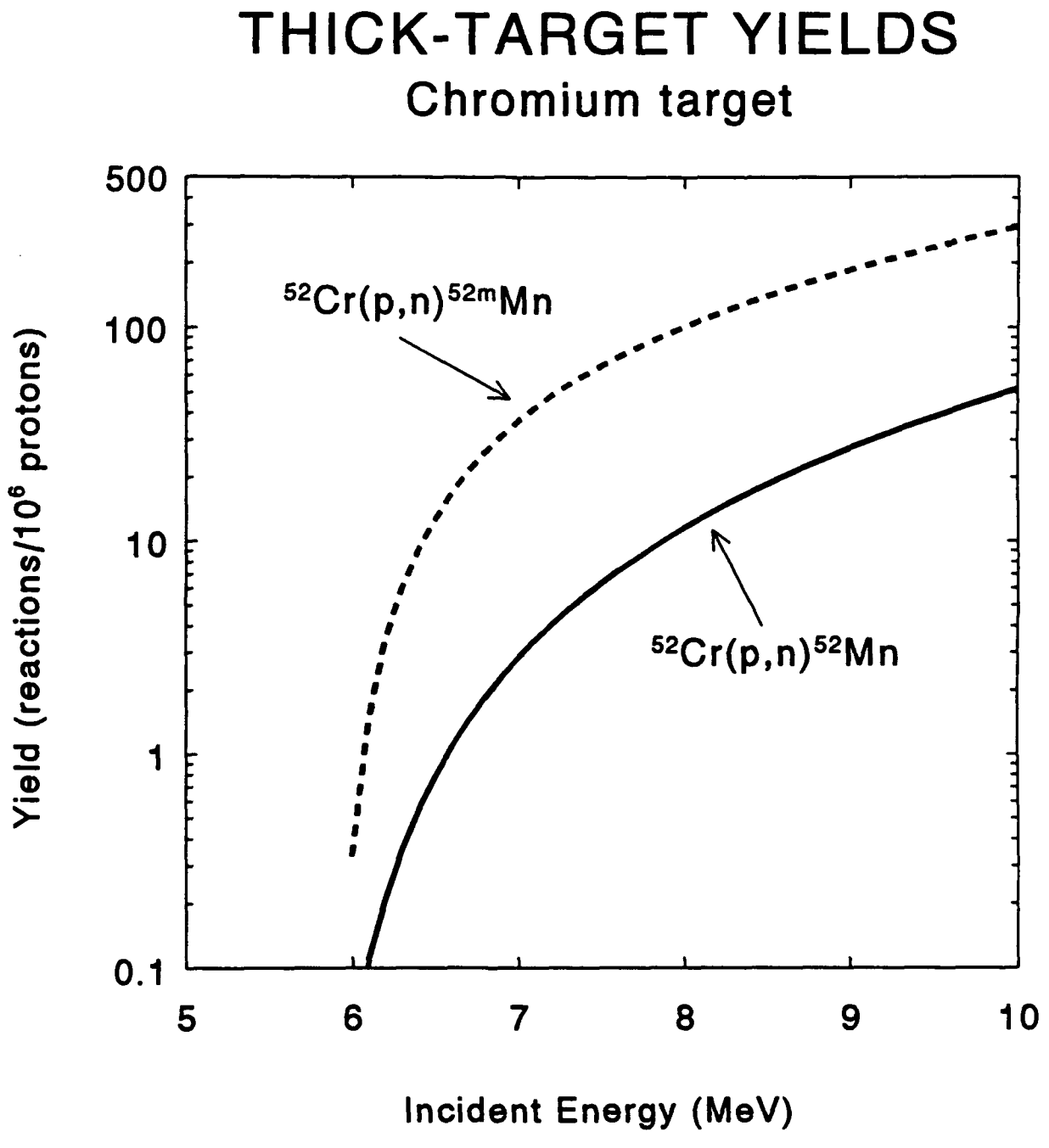

Fig. 7. Thick-target yields for the $^{52}Cr(p,n)^{52}Mn$ and $^{52}Cr(p,n)^{52m}Mn$ reactions in a natural chromium target.

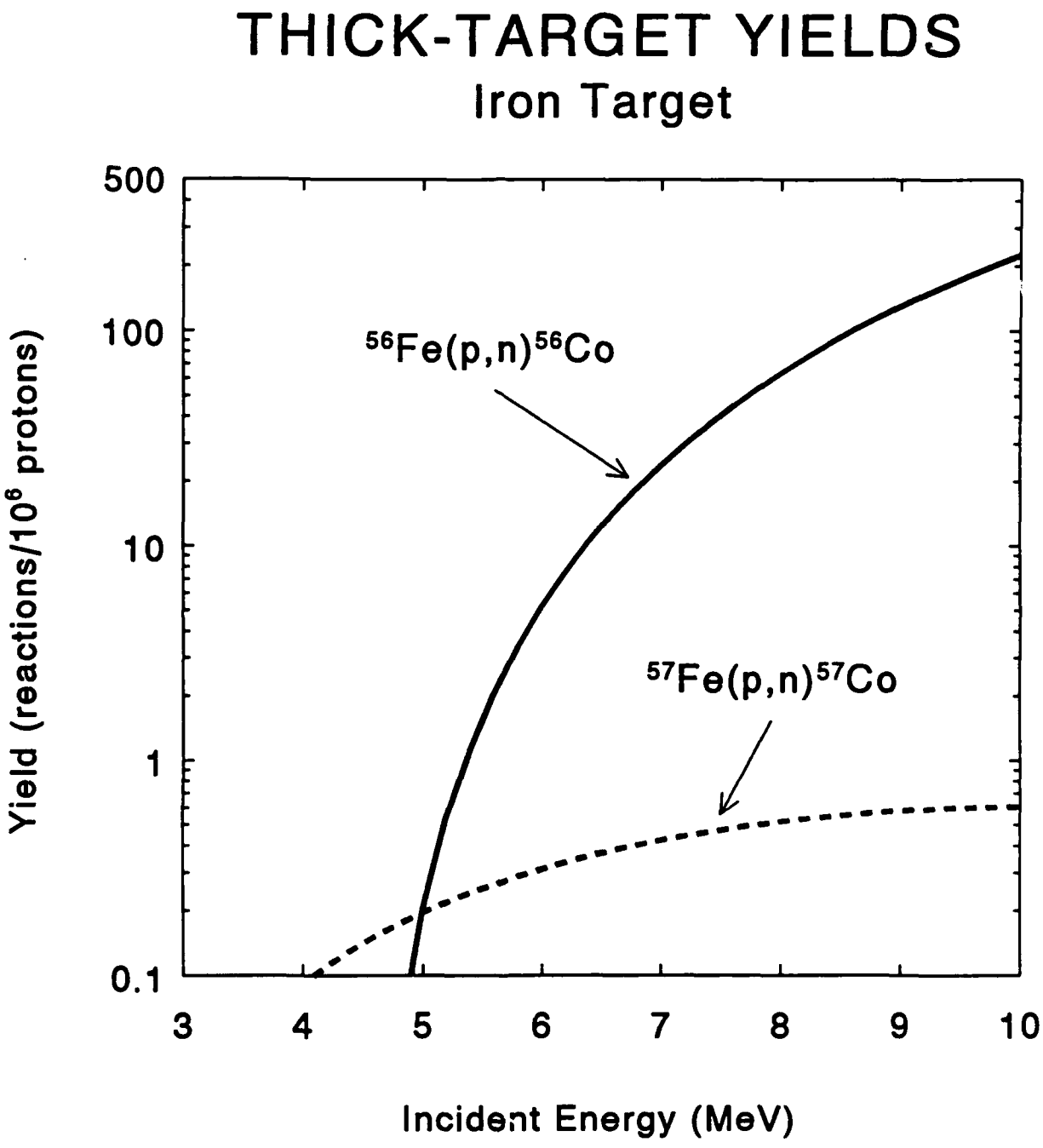

Fig. 8. Thick-target yields for the $^{56}Fe(p,n)^{56}Co$ and $^{57}Fe(p,n)^{57}Co$ reactions in a natural iron target.

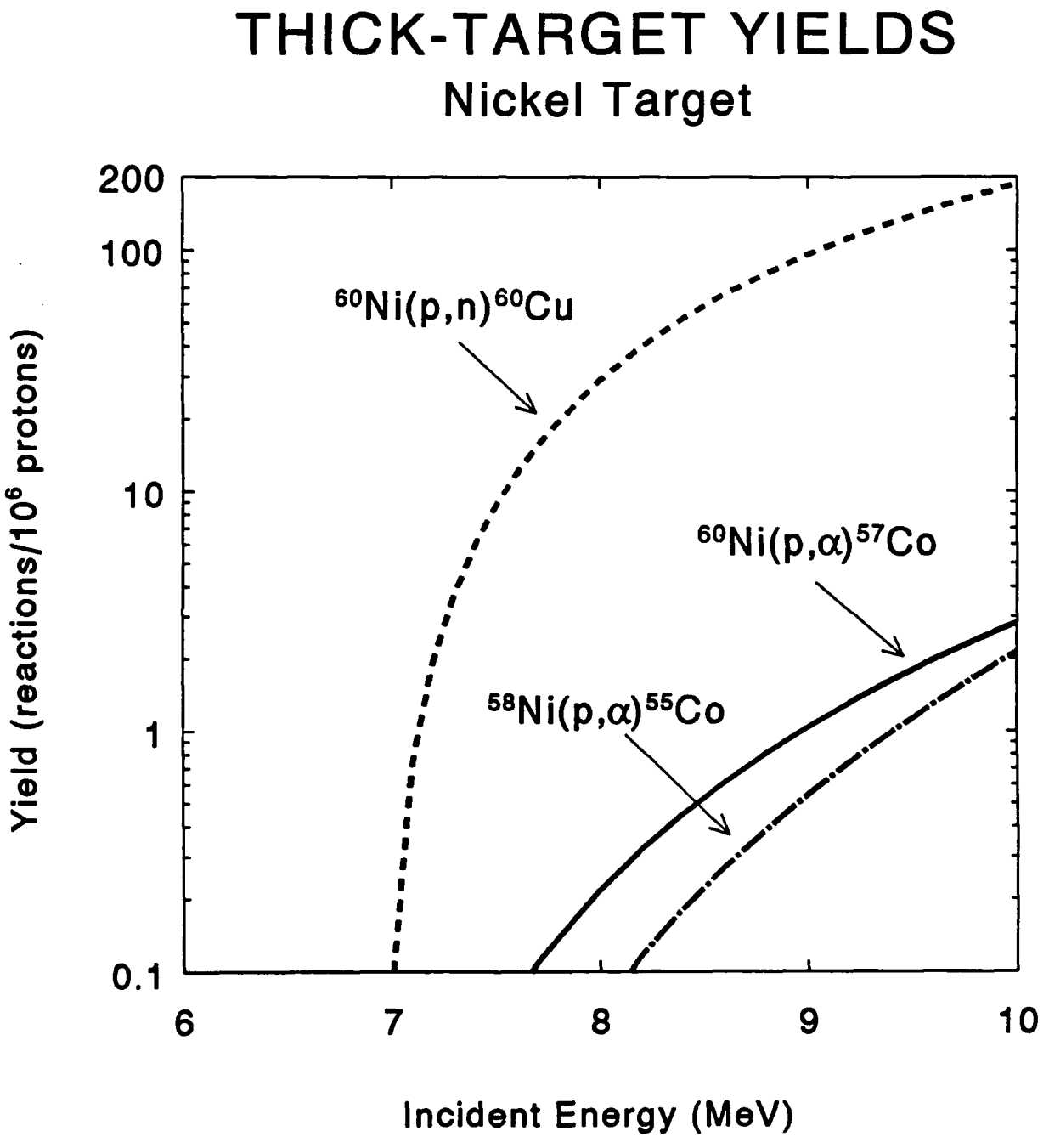

Fig. 9. Thick-target yields for the $^{60}Ni(p,n)^{60}Cu$, $^{60}Ni(p,\alpha)^{57}Co$, and $^{58}Ni(p,\alpha)^{55}Co$ reactions in a natural nickel target.

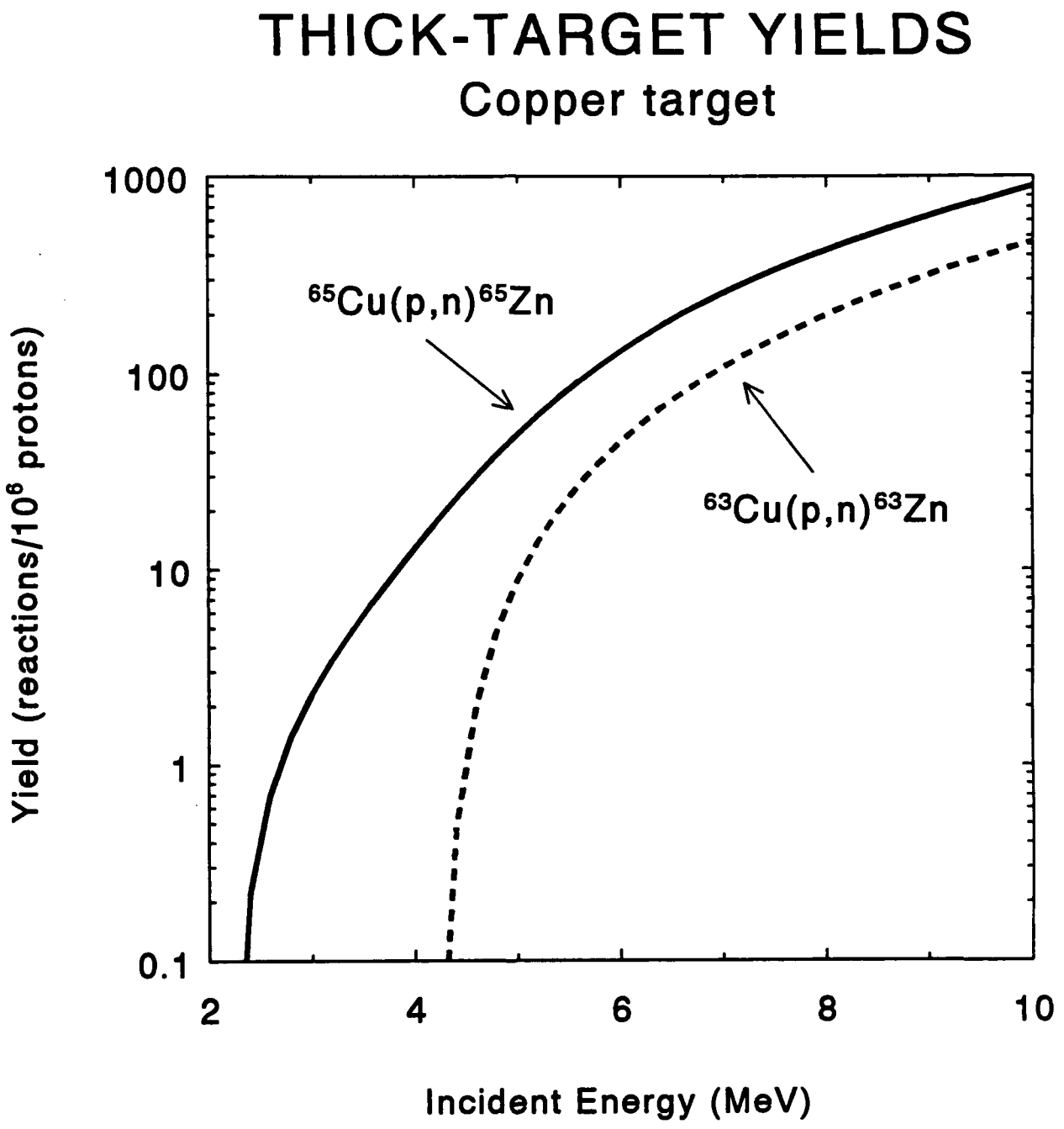

Fig. 10. Thick-target yields for the $^{65}Cu(p,n)^{65}Zn$ and $^{63}Cu(p,n)^{63}Zn$ reactions in a natural copper target.

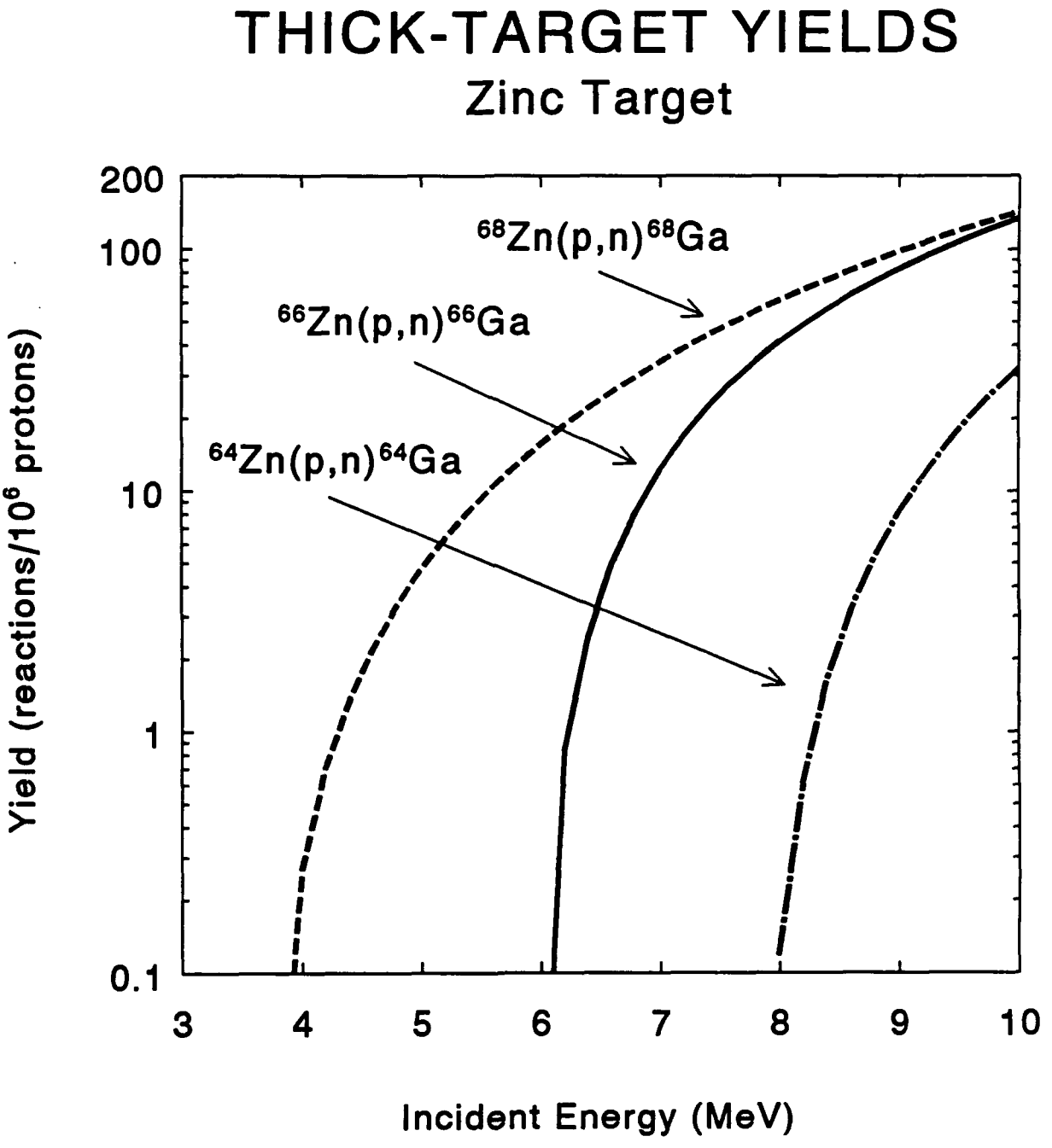

Fig. 11. Thick-target yields for the $^{64}Zn(p,n)^{64}Ga$, $^{66}Zn(p,n)^{66}Ga$, and $^{68}Zn(p,n)^{68}Ga$ reactions in a natural zinc target.

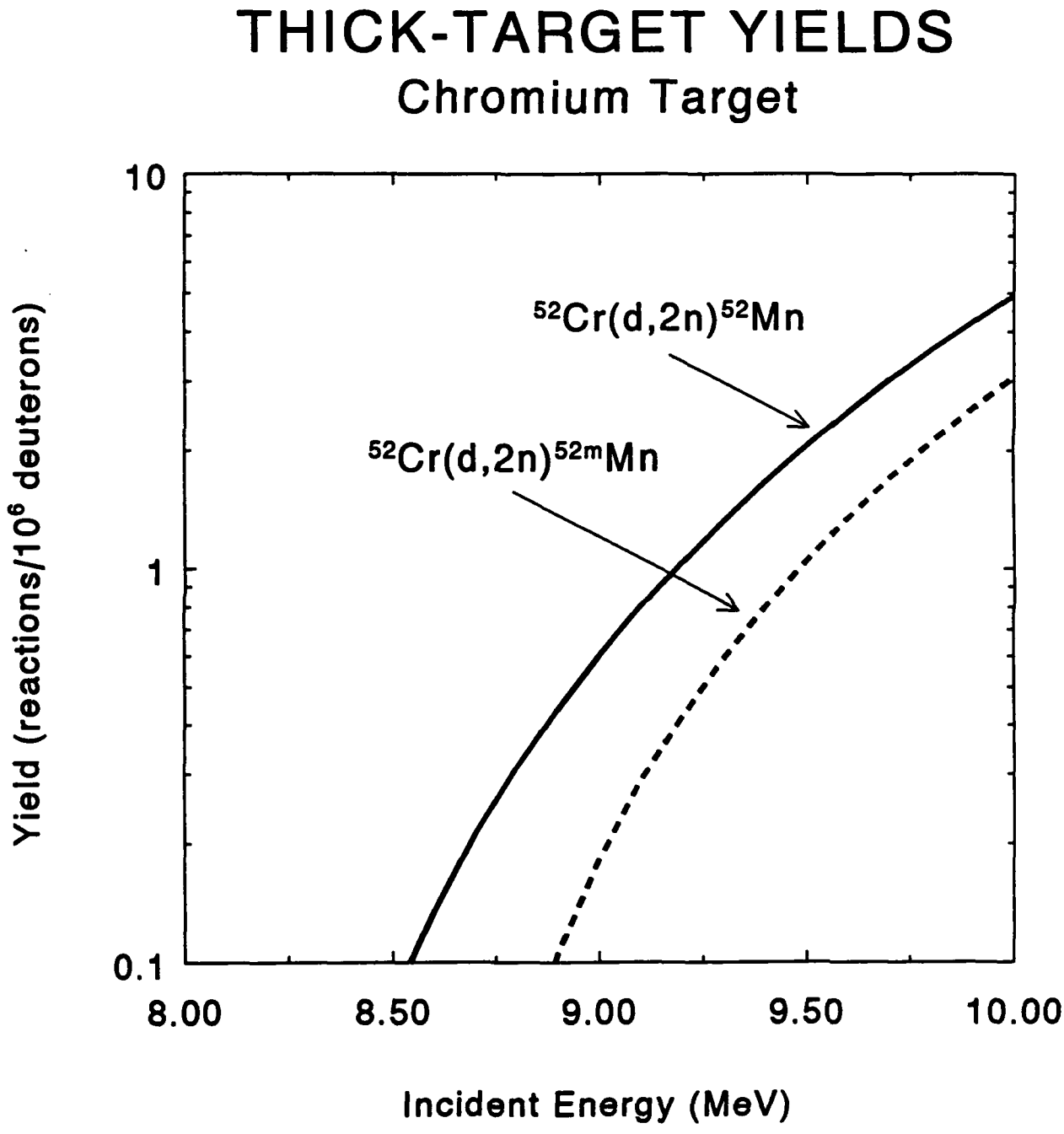

Fig. 12. Thick-target yields for the $^{52}Cr(d,2n)^{52}Mn$ and $^{52}Cr(d,2n)^{52m}Mn$ reactions in a natural chromium target.

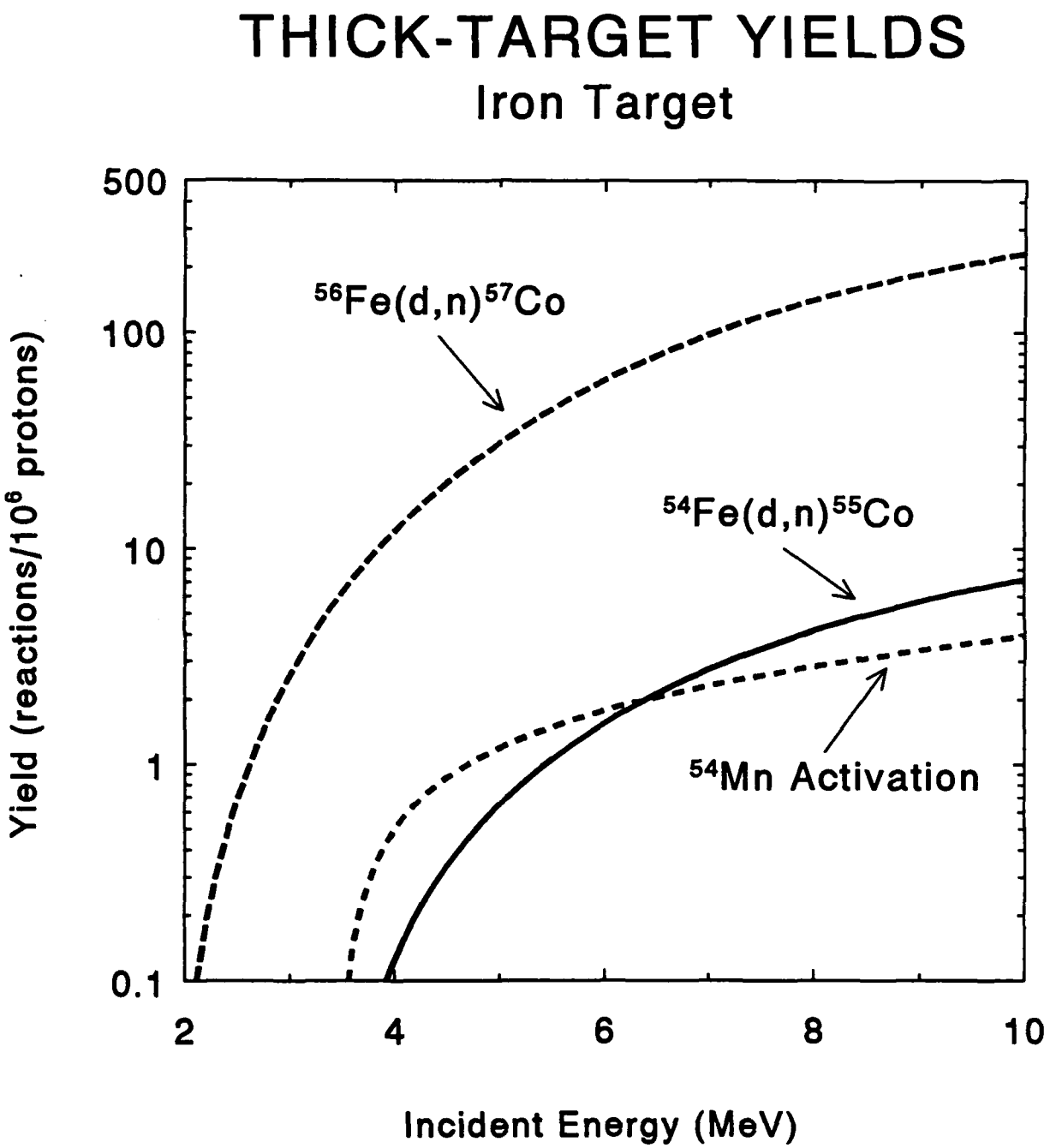

Fig. 13. Thick-target yields for the $^{56}Fe(d,n)^{57}Co$ and $^{54}Fe(d,n)^{55}Co$ reactions and for the activation of ^{54}Mn by deuterons on a natural iron target.

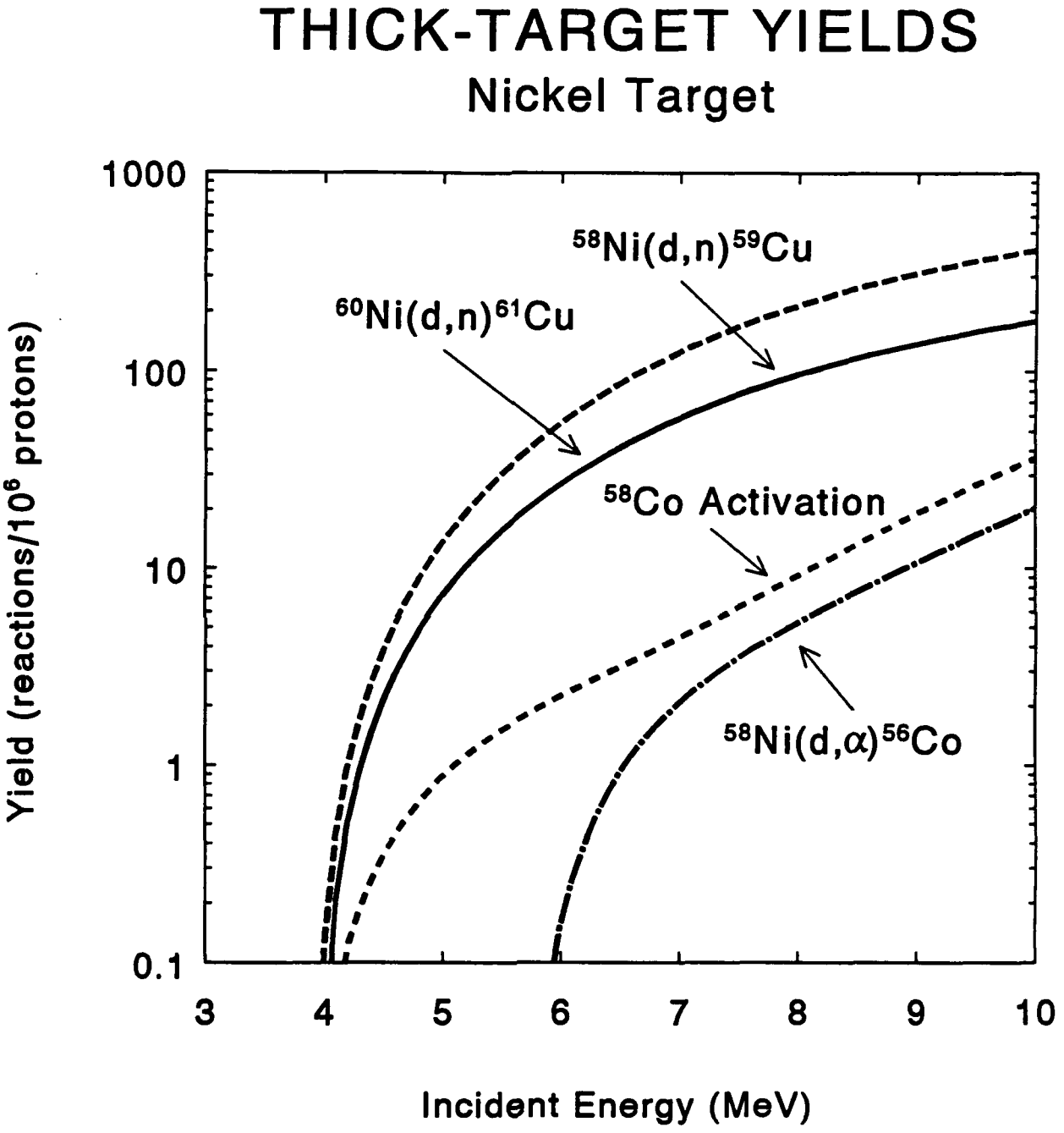

Fig. 14. Thick-target yields for the $^{58}Ni(d,n)^{59}Cu$, $^{60}Ni(d,n)^{61}Cu$, and $^{58}Ni(d,\alpha)^{56}Co$ reactions and for the activation of ^{58}Co by deuterons on a natural nickel target.

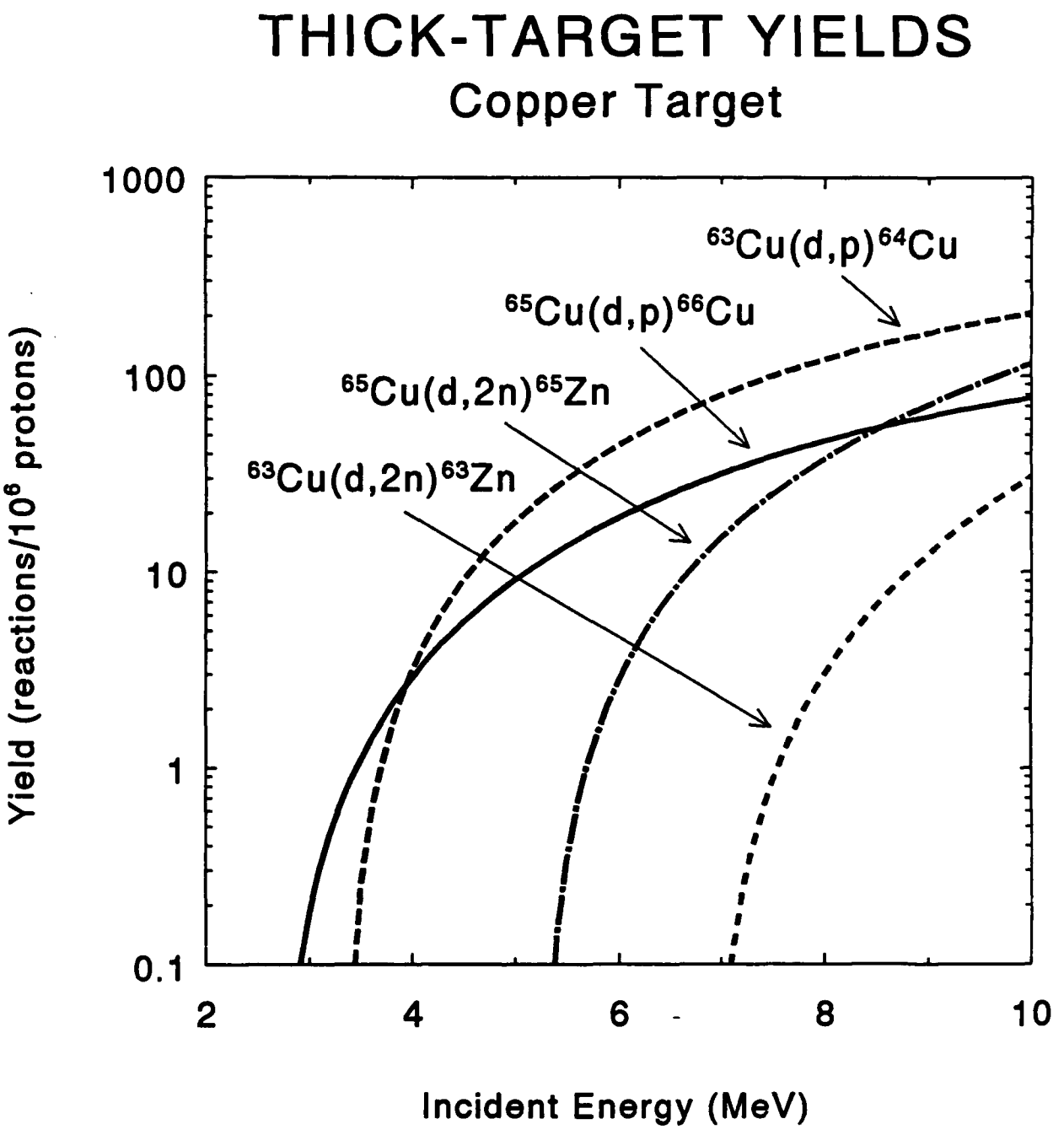

Fig. 15. Thick-target yields for the $^{63}Cu(d,p)^{64}Cu$, $^{65}Cu(d,p)^{66}Cu$, $^{63}Cu(d,2n)^{63}Zn$, and $^{65}Cu(d,2n)^{65}Zn$ reactions in a natural copper target.

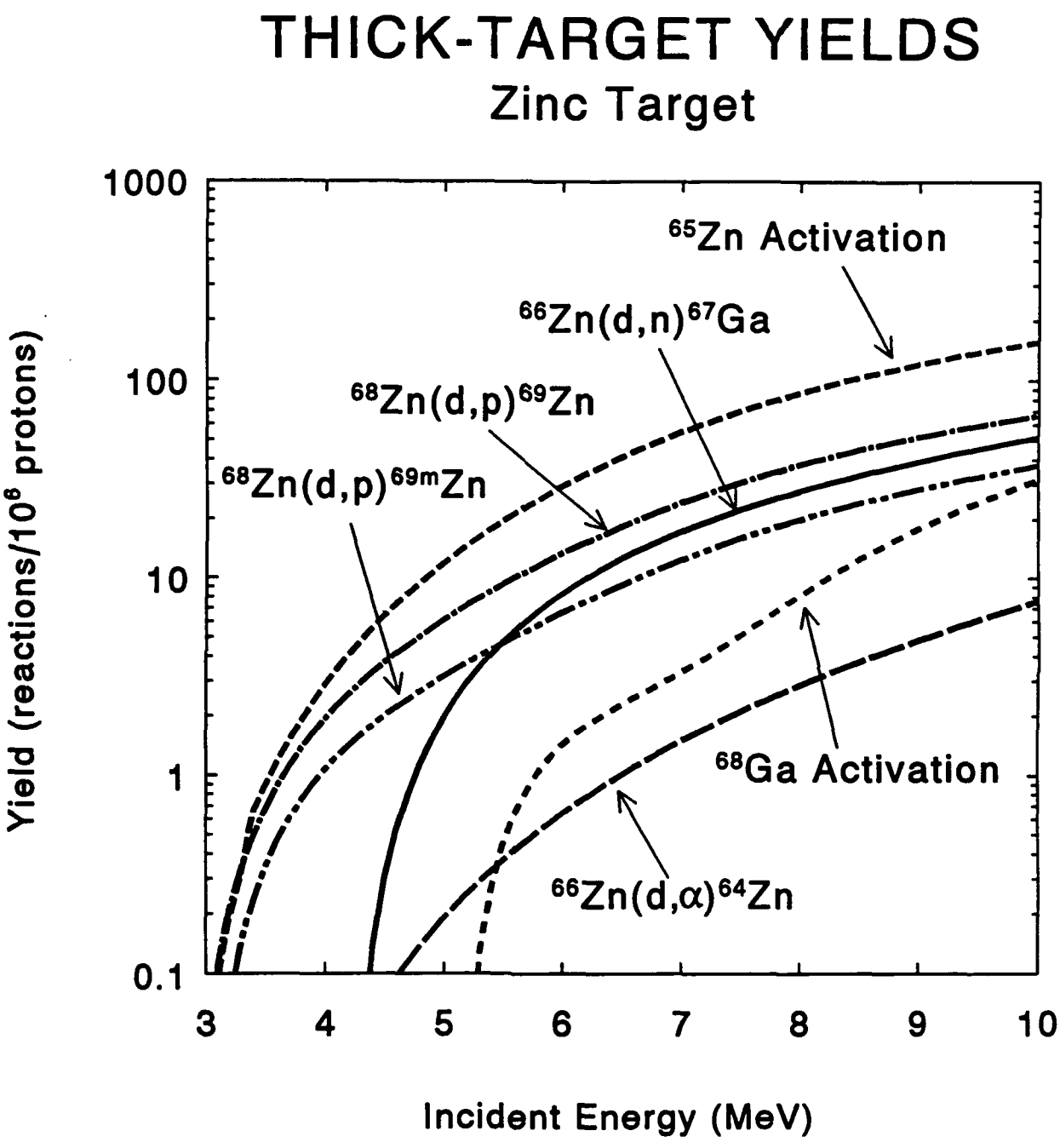

Fig. 16. Thick-target yields for the activation of ^{65}Zn by deuterons and for the $^{66}Zn(d,n)^{67}Ga$, $^{68}Zn(d,p)^{69}Zn$, $^{68}Zn(d,p)^{69m}Zn$, $^{66}Zn(d,\alpha)^{64}Cu$, and $^{68}Zn(d,2n)^{68}Ga$ reactions in a natural zinc target.